Available online at www.sciencedirect.com
SCIENCE DIRECT®
ELSEVIER
International Journal of Coal Geology 55 (2003) 225–259
International Journal of COAL GEOLOGY
www.elsevier.com/locate/ijcoalgeo

Petrography and geochemistry of Carboniferous coal seams in the Donets Basin (Ukraine): implications for paleoecology

R.F. Sachsenhofer[a,*], V.A. Privalov[b], A. Izart[c], M. Elie[c], J. Kortensky[d], E.A. Panova[e], A. Sotirov[a], M.V. Zhykalyak[f]

[a] *Abt. Mineralogie und Petrologie, Institut für Geowissenschaften, Montanuniversität Leoben, Peter-Tunner-Strasse 5, A-8700 Leoben, Austria*
[b] *Donetsk National Technical University, Artem str. 58, UA-83000 Donetsk, Ukraine*
[c] *UMR 7566G2R, Université Henri Poincaré, BP239, F-54506, Vandoeuvre-les-Nancy, France*
[d] *University of Mining and Geology "St. Ivan Rilski", BG-1700 Sofia, Bulgaria*
[e] *UkrNIMI, National Academy of Science of Ukraine, Tchelyuskintsev str. 291, UA-83121 Donetsk, Ukraine*
[f] *Donetsk State Regional Geological Survey, Sybirtseva str. 17, UA-84500 Artemovsk, Ukraine*

Received 6 January 2003; accepted 12 June 2003

Abstract

The Carboniferous succession in the Donets Basin hosts about 130 seams, each with a thickness over 0.45 m. Nine economically important seams from the (south)western Donets Basin are studied using organic petrographical, inorganic geochemical, and organic geochemical techniques. The main aim of the study is the reconstruction of peat facies of Serpukhovian (Mississippian) and Moscovian (Middle Pennsylvanian) coals.

Formation of major coal seams commenced during Serpukhovian times. Early Serpukhovian coal accumulated in a relatively narrow shore-zone and is rich in inertinite and liptinite. Very low ash yields, low to moderate sulphur contents, and upward increasing inertinite contents suggest coal deposition in raised mires.

Moscovian coal has a significantly wider lateral extension and is generally rich in vitrinite. Coal properties vary widely in response to different peat facies. Low-sulphur, low-ash k_7 coal was formed in a raised mire or in a low-lying mire without detrital input. l_1 and l_3 seams containing several fluvial partings were formed in low-lying mires. Both seams are more than 2 m thick. Seams m_2 and m_3 contain high-sulphur coal, a consequence of deposition in a peat with marine influence. In contrast, syngenetic sulphur content is low in the $m_5^{1\ upper}$ seam, which was formed in a lacustrine setting. The late Moscovian n_1 seam, up to 2.4 m thick, accumulated in a swamp with a vegetation rich in bryophytes and pteridophytes. The properties of the n_1 seam are transitional between those of Serpukhovian and other Moscovian seams. Differences in maceral composition between Serpukhovian and Moscovian coals probably reflect changes in climate and vegetation type.

Tuff layers are observed in the l_1, l_3, and m_3 seams. The l_3 and m_3 seams contain abundant authigenic quartz. Trace element contents are high in many seams. As contents are especially high in seams c_{10}^2, k_7, l_3 and m_3. Ash in the l_3 seam contains up to 8000 ppm As. Co is enriched near the base of several seams. Maxima up to 2400 ppm occur in the ash of the k_7 and l_3 seams. Cd contents in ash are frequently as high as 30 or 40 ppm.

Keywords: Ukraine; Coal; Serpukhovian; Moscovian; Organic geochemistry; Inorganic geochemistry; Coal petrography

* Corresponding author. Fax: +43-3842-402-9902.
E-mail address: sachsenh@unileoben.ac.at (R.F. Sachsenhofer).

0166-5162/03/$ - see front matter © 2003 Elsevier B.V. All rights reserved.
doi:10.1016/S0166-5162(03)00112-5

1. Introduction

The Donets Basin (Donbas), located mainly in the Ukraine with the eastern part of the basin extending into Russia, contains one of the major coal fields in the world. The basin covers an area of 60,000 km^2 and is located between the Dniepr–Donets Basin and the buried Karpinsky Swell (Fig. 1).

The Carboniferous succession in the Donets Basin hosts about 130 seams, each with a thickness over 0.45 m. Total coal thickness is about 60 m (Ritenberg, 1972). The coal is generally of meta-anthracite rank in the central part of the basin. Low-rank coals are restricted to the western and northern basin margins (Fig. 1; Levenshtein et al., 1991a). The thickness of coal seams currently mined is in the range of 0.6 to 2.5 m. Seams in excess of 2 m are rare. Proven commercial reserves in the Ukrainian part in the depth interval up to 1600–1800 m are 52 Gt (Zhykalyak and Privalov, 2002).

The average methane content of coal is 14.7 m^3/t (Marshall et al., 1996), but numerous seams have significantly higher gas content, presenting a high potential for coal mine methane projects (e.g. Triplett et al., 2001). On the other hand, the high methane content presents a severe mine safety problem in this area.

In the present paper, some of the economically most important seams are studied using a multidisciplinary approach involving organic petrographical, inorganic geochemical, and organic geochemical techniques. The main aim of the study is to reconstruct the depositional environment of the seams. In addition, differences between Mississippian (Serpukhovian) and middle Pennsylvanian (Moscovian) peat forming environments are investigated. Inorganic geochemical analyses are applied mainly to support the characterization of the mineral matter in the coal. However, because Donets coals are known to be rich in hazardous trace elements such as Hg, As, Cd, Pb, and Zn (Panov et al., 1999; Kizilshtein and Kholodkov, 1999), selected trace elements are included in the present study.

2. Geological setting

The Donets Basin forms part of the Pripyat–Dniepr–Donets–Karpinsky Basin (Fig. 1), a Late Devonian rift structure located on the southern part of the Eastern European craton (Stovba and Stephenson, 1999; Stephenson et al., 2001). Some important aspects of the evolution of the basin are summarized in Fig. 2. Total thickness of Devonian pre- and syn-rift rocks is 750 m at the margins of the Donets Basin, but may reach 5 km towards the basin center.

Major post-rift subsidence occurred during the Permo-Carboniferous. The Carboniferous sequence, up to 14 km thick, is subdivided into lithostratigraphic units named suites A, B, C, to P (Lutugin and Stepanov, 1913). Their correlation with the standard time-scale is presented in Fig. 2. A sequence stratigraphic frame for the Permo-Carboniferous rocks in this basin is provided by Izart et al. (1996, 1998, 2002a). The coal-bearing succession consists of elementary sequences, composed of fluvial sandstone, coal, marine limestone or claystone, and deltaic claystone and siltstone (Izart et al., 2002b). The percentage of continental deposits is higher in the western than in the eastern Donets Basin. Coal seams and intercalations of coal are present throughout the Carboniferous succession. However, lower Serpukhovian (suite C) and Moscovian successions (suites K to M) are especially rich in coal (Levenshtein et al., 1991b).

Economic coal seams of suite C are mainly found in a narrow (~ 10 km wide), NW–SE trending zone along the southwestern basin margin (Shulga, 1981). Moscovian seams have a significantly wider areal extent, with some seams covering the entire Donets Basin. A detailed stratigraphic column of Moscovian rocks, together with a number code for limestone layers (capital letters) and coal seams (small letters), is shown in Fig. 2.

Permian rocks are preserved along the western and northern basin margins, where they are represented by a sandstone-mudstone series with limestone interbeds (Nesterenko, 1978). Thick evaporites occur in Asselian and Sakmarian levels. Only relatively thin sediments were deposited during the Mesozoic and Cenozoic.

The structure of the Donbas Foldbelt, which is the inverted part of the Dniepr–Donets Basin, is dominated by WNW–ESE striking anticlines and synclines. The maturity of the Carboniferous rocks increases from the western and northern basin margins

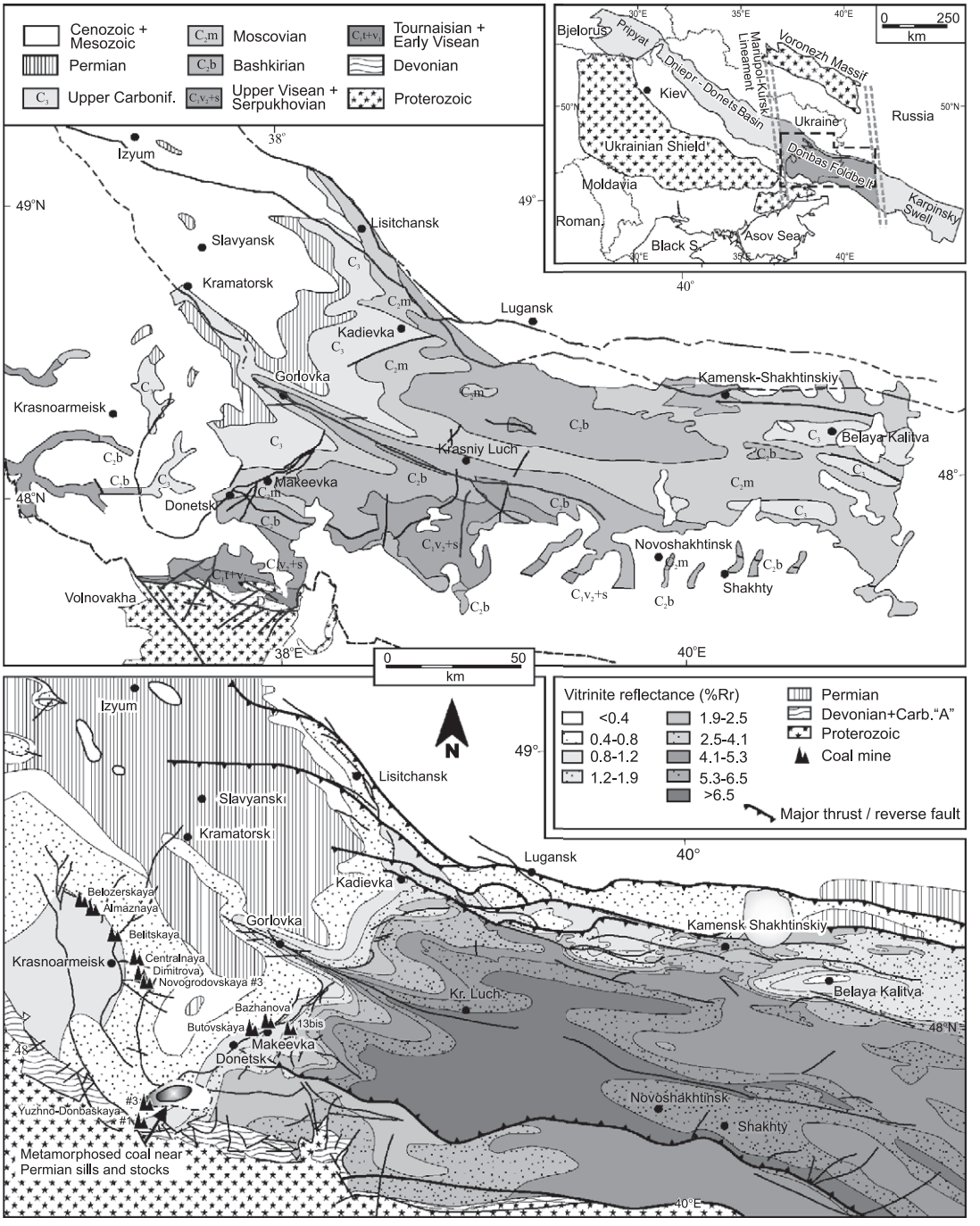

Fig. 1. Geologic sketch map of the Donets Basin (modified after Popov, 1963), and coalification map at the top of the Carboniferous sequence (modified after Levenshtein et al., 1991a). Eight coal seams from mines in the (south)western Donets Basin were studied. The position of the mines is shown in the vitrinite reflectance map.

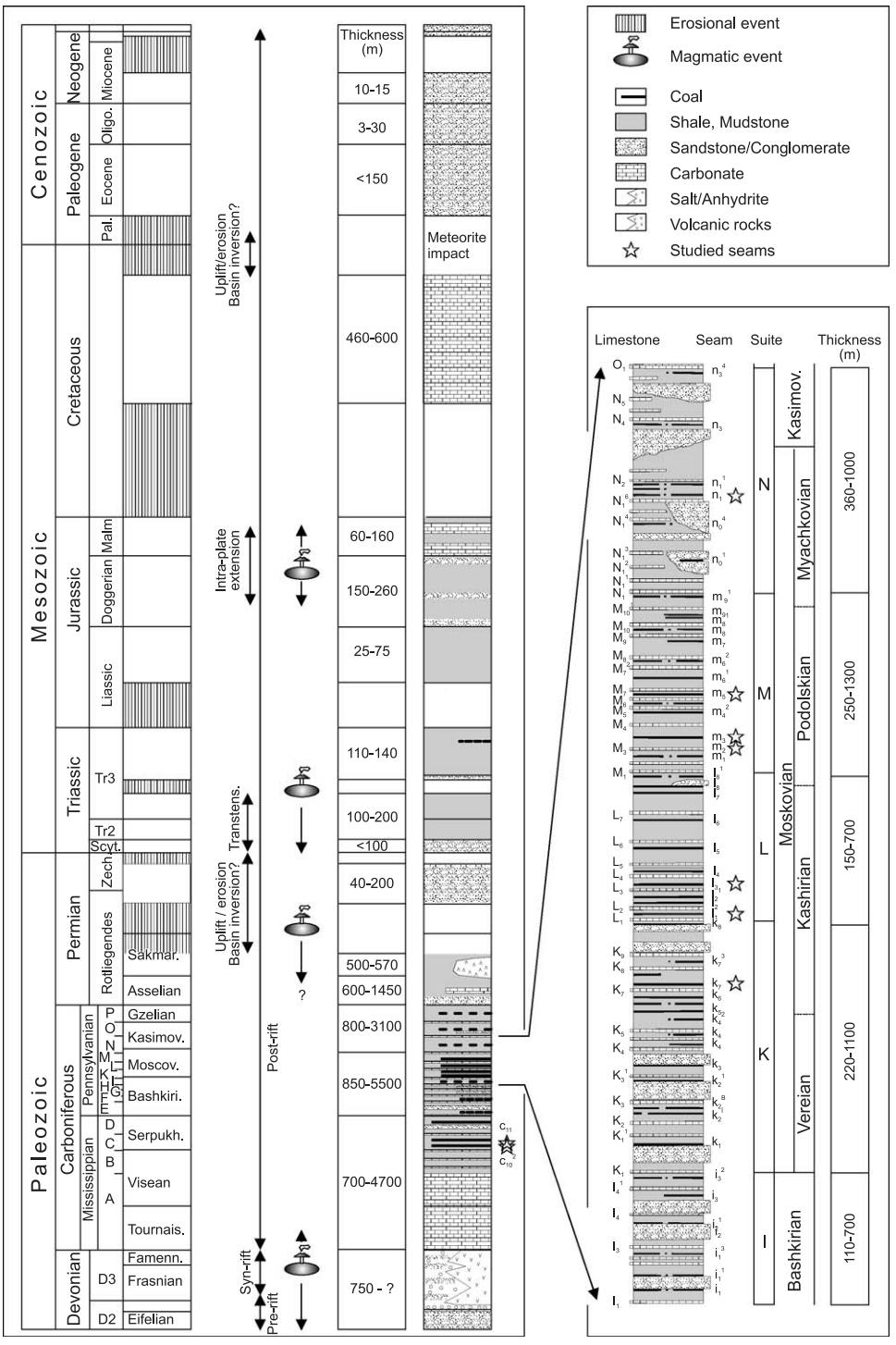

Fig. 2. Chrono- and lithostratigraphy of the Donets Basin. Major magmatic and tectonic events are shown (Sterlin et al., 1963; Belokon, 1971; Einor, 1996; Privalov et al., 1998; Stovba and Stephenson, 1999). A detailed stratigraphic column is provided for the Moscovian sequence.

towards the basin center and mirrors the main structural elements (Fig. 1). The rank of the coals is controlled mainly by temperatures attained during deep Permian burial. The resulting coalification pattern was overprinted in some areas by thermal events probably related to late Permian magmatic intrusions (Sachsenhofer et al., 2002).

3. Samples and methods

Eleven profiles representing eight Serpukhovian and Moscovian seams, each with a thickness in excess of 1 m, were selected for the investigation. In order to investigate low rank coals, the seam profiles were sampled in the (south-)western part of the Donets Basin (Krasnoarmeisk, Donetsk-Makeevka, Yuzhno-Donbasskaya regions; Fig. 1). Most coals are high volatile bituminous (0.60–0.92% Rr); two profiles contain medium volatile bituminous coal (1.2% and 1.4% Rr).

The present study is based on 71 samples, taken by staff of the coal mines, who also logged the seam sections. Only four samples are from Serpukhovian seams: three samples represent the lower, middle, and upper part of the c_{10}^{2} seam, respectively, and a single channel sample represents the entire c_{11} seam. Each Moscovian seam section is represented by 5 to 11 samples. Each sample typically represents a 10-cm interval.

As a first step, the samples were crushed to a maximum grain size of 3 mm. For petrographical investigations, a representative part of the sample was mounted in epoxy resin, ground and polished. At least 300 points were counted on polished sections using a Leitz microscope in reflected white and fluorescent light to provide data for maceral analyses. The maceral abundances refer to percentages on a mineral matter free basis (% mmf).

There have been several suggestions to characterize coal facies on the basis of maceral ratios (e.g. Diessel, 1986; Calder et al., 1991). These maceral indexes were developed for specific coals of Permian and Pennsylvanian ages and do not necessarily extrapolate to other coals, even of the same age. Moreover, modern peats studies show that maceral ratios alone are of limited utility to interpret depositional environments (e.g. Dehmer, 1995; Wüst et al., 2001; Moore and Shearer, 2003). Even so, maceral ratios provide a convenient way to present complex maceral data. Therefore, the following indexes were calculated for samples with ash yields $< 50\%$.

The gelification index (GI; Diessel, 1986) contrasts gelified with fusinitised macerals. The GI is considered to give an indication of the relative dryness of peat forming conditions, although pyrofusinite may be blown or washed into the system.

$$\mathrm{GI} = \frac{\text{vitrinite} + \text{macrinite}}{\text{fusinite} + \text{inertodetrinite}}$$

The groundwater index (GWI; Calder et al., 1991) is the ratio of strongly gelified vitrinite plus detrital mineral matter to weakly gelified vitrinite. Because gelocollinite and corpocollinite are generally rare, the GWI is mainly a measure for the detrital input.

$$\mathrm{GWI} = \frac{\text{gelocollinite} + \text{corpocollinite} + \text{detrital mineral matter}}{\text{telinite} + \text{telocollinite} + \text{desmocollinite}}$$

The vegetation index (VI; Calder et al., 1991) contrasts macerals of forest affinity with those of herbaceous and aquatic affinity.

$$\mathrm{VI} = \frac{\text{telinite} + \text{telocollinite} + \text{fusinite} + \text{semifusinite} + \text{suberinite} + \text{resinite}}{\text{desmocollinite} + \text{vitrodetrinite} + \text{inertodetrinite} + \text{alginite} + \text{liptodetrinite} + \text{sporinite} + \text{cutinite}}.$$

Table 1
Position above the base of the seam, ash yield, total sulphur and organic carbon contents (TOC), Rock Eval parameters (T_{max}, S1 [mgHC/g Rock], hydrogen index [HI; mgHC/gTOC]), maceral composition (V: vitrinite; L: liptinite; I: inertinite), and facies indicators (GWI: groundwater index; VI: vegetation index; GI: gelification index) for Donets Basin samples

Sample	Dist. from base (m)	Ash	Sulph. % db	TOC	Rr %	T_{max} °C	S1	HI	V	L % mmf	I	MM	Pyr.	Facies Indicators GWI	VI	GI
n_1 (Butovskaya)																
5	1.25	4.3	2.9	77.4	0.63	436	9.7	306	72	13	15	2	2	0.04	1.0	5.5
4	0.9	11.6	1.5	75.5	0.75	438	6.6	244	56	12	32	1	0	0.02	0.7	1.7
3	0.5	2.0	1.2	82.0	0.79	444	6.5	262	73	11	16	1	1	0.02	0.6	4.6
2	0.2	6.9	1.4	77.9	0.83	442	6.3	255	82	6	12	1	0	0.03	0.7	7.2
1	0.01	9.5	1.7	75.7	0.84	437	6.3	254	82	8	10	2	1	0.04	1.0	8.9
$m_5^{1\ upper}$ (Almaznaya)																
5	0.9	1.4	1.1	81.7	0.72	432	1.7	223	75	8	17	0	0	0.02	0.7	4.4
4	0.6	14.2	7.3	65.5	0.75	435	0.9	185	91	3	6	5	5	0.06	2.4	15.5
3	0.3	2.5	2.0	78.4	0.72	436	1.5	210	72	9	19	0	0	0.01	1.6	3.8
2	0.01	1.3	1.3	79.9	0.73	435	1.9	246	79	7	14	1	0	0.02	1.0	5.7
m_3 (Bazhanova)																
10	1.5	36.1	4.0	54.8	1.17	477	7.5	163	100	0	0	16	3	0.19	1.5	100
8	1.4	2.8	2.4	86.8	1.23	476	12.8	149	89	0	11	1	1	0.01	0.6	8.0
7	1.2	2.9	4.1	86.8	1.23	477	8.9	150	80	0	20	2	2	0.02	1.1	4.0
6	1	3.1	4.1	83.9	1.15	465	9.2	170	91	0	9	5	5	0.05	1.7	10.5
5	0.8	47.2	3.2	48.0	1.21	480	7.9	146	85	0	15	25	4	0.05	2.5	5.7
4	0.6	8.7	7.3	78.0	1.10	477	9.6	155	84	0	16	6	5	0.08	0.2	5.3
3	0.4	0.9	0.5	89.3	1.20	481	9.3	148	80	0	20	0	0	0.00	1.0	4.1
2	0.2	8.6	7.3	81.1	1.13	480	9.4	144	78	0	22	6	6	0.09	0.3	3.6
1	0.01	42.6	4.1	50.6	1.17	479	6.4	179	100	0	0	23	6	0.56	1.1	100
m_2 (Belitskaya)																
7	1.05	20.0	4.8	63.2	0.64	435	3.0	264	73	17	11	12	8	0.20	0.7	6.8
6	0.95	6.7	3.9	74.3	0.65	438	7.1	285	83	6	11	5	4	0.07	0.9	7.4
5	0.75	4.7	3.9	76.7	0.67	434	4.5	284	85	6	10	4	4	0.05	1.2	8.8
4	0.55	89.1	0.4	3.2	0.69	441	0.2	182	100	0	0	96	0			
3	0.35	12.0	2.3	71.2	0.73	432	3.0	271	79	6	15	3	1	0.05	0.7	5.4
2	0.2	17.6	8.0	64.4	0.71	429	4.8	298	86	7	6	8	2	0.12	1.2	14.0
1	0.01	21.2	8.0	61.7	0.71	433	3.9	290	87	7	6	15	6	0.22	1.4	15.6
l_3 (Almaznaya)																
11	1.95	9.6	1.1	77.7	0.87	445	4.3	207	79	7	14	0	0	0.01	1.4	5.7
10	1.55	1.4	1.0	85.0	0.88	446	2.7	200	75	7	18	0	0	0.00	0.9	4.4
9	1.2	2.6	1.9	83.6	0.86	445	1.9	212	80	6	13	1	1	0.02	1.5	5.9
8	0.85	1.8	1.3	83.6	0.91	449	2.6	200	89	5	6	0	0	0.00	1.7	15.2
7	0.55	35.6	0.7	54.4	0.90	446	2.3	212	88	7	5	21	0	0.57	0.8	18.6
6	0.1	5.1	1.5	79.7	0.90	448	3.7	216	81	12	7	0	0	0.00	0.9	11.0
l_3 (Belozerskaya)																
12	2.25	7.4	2.0	78.7	0.81	444	7.2	209	82	6	12	1	1	0.02	1.6	6.8
10	1.85	3.4	2.3	80.4	0.81	445	11.3	241	68	12	20	1	1	0.01	1.4	3.4
9	1.65	9.7	4.5	76.9	0.89	443	7.1	203	71	5	24	1	1	0.01	1.7	2.9
8	1.5	67.5	1.7	24.2	0.83	442	3.0	257	85	4	11	62	3			
7	1.35	24.3	2.9	65.6	0.82	439	6.2	248	81	7	12	16	2	0.29	0.7	6.5
6	1.15	85.0	1.2	7.0	0.80	443	0.8	234	84	0	16	90	0			
5	1	4.9	3.7	79.5	0.82	446	8.4	222	76	12	13	3	3	0.05	1.2	6.0
4	0.8	63.5	0.8	23.8	0.82	446	2.9	228	89	5	6	56	2			

Table 1 (*continued*)

Sample	Dist. from base (m)	Ash	Sulph. % db	TOC	Rr %	T_{max} °C	S1	HI	V	L % mmf	I	MM	Pyr.	Facies Indicators GWI	VI	GI
l_3 (Belozerskaya)																
3	0.6	11.6	2.1	73.7	0.85	441	7.0	229	86	9	5	3	1	0.04	1.4	16.0
2	0.4	1.5	2.0	81.8	0.84	447	10.5	214	81	14	5	1	1	0.01	1.1	16.1
1	0.1	3.4	3.1	81.9	0.87	445	8.7	217	86	7	6	3	3	0.03	1.9	13.7
l_1 (Dimitrova)																
9	1.87	9.3	5.7	73.1	0.71	442	7.4	245	67	9	24	5	5	0.12	1.1	2.8
8	1.72	10.0	3.3	77.1	0.72	443	8.6	224	70	7	22	5	1	0.11	1.0	3.2
7	1.41		1.0	1.7		445	0.1	88								
6	1.15	2.3	3.6	81.1	0.74	442	14.7	242	78	7	15	0	0	0.01	1.1	5.1
5	0.94	1.4	3.4	83.8	0.73	442	9.6	248	71	11	18	1	1	0.06	0.9	4.1
4	0.73	13.5	2.9	71.0	0.76	441	6.6	250	73	10	18	6	1	0.11	1.0	4.2
3	0.52	4.1	5.5	80.1	0.77	439	11.8	263	83	11	6	1	1	0.02	1.0	14.6
2	0.31	3.3	3.5	81.9	0.76	440	11.5	253	81	11	8	2	2	0.03	1.4	10.1
1	0.1	8.3	7.4	75.3	0.74	438	8.6	248	80	6	15	8	8	0.14	1.5	5.4
l_1 (Novogrodovskaya)																
6	1.77	60.3	1.6	28.7	0.73	429	2.2	242	90	2	8	56	1			
5	1.42	54.4	2.4	31.4	0.76	429	3.7	258	98	1	1	54	1			
4	1.11	4.7	4.2	76.5	0.69	435	8.9	257	79	9	11	2	2	0.03	0.8	7.0
3	0.75	2.9	4.0	77.7	0.71	437	7.5	244	85	12	3	1	1	0.01	0.7	26.2
2	0.4	4.9	5.3	76.9	0.72	432	5.6	231	80	9	11	3	3	0.04	1.8	7.2
1	0.19	29.3	2.5	51.9	0.73	432	5.6	276	59	15	25	12	2	0.30	0.6	2.3
l_1 (13-bis)																
7	1.09	87.6	1.0	5.5	1.32	495	0.3	49	100	0	0	94	1			
6	0.79	4.6	3.1	84.1	1.34	488	3.3	120	86	0	13	4	4	0.04	1.4	6.4
5	0.6	48.9	1.8	45.8	1.37	484	1.4	124	83	1	16	27	1	0.70	1.1	5.4
4	0.46	4.0	3.1	85.4	1.38	489	2.5	123	79	0	21	2	2	0.03	1.4	3.8
2	0.29	6.1	3.4	83.5	1.47	490	2.2	119	88	0	12	3	3	0.04	1.1	7.2
1	0.05	5.3	3.2	84.3	1.44	489	2.7	121	84	0	16	4	4	0.05	1.5	5.4
k_7 (Centralnaya)																
5	0.9	4.4	2.3	81.1	0.95	445	7.7	221	78	15	7	0	0	0.00	0.9	10.8
4	0.7	0.7	0.9	84.2	0.91	447	7.6	236	89	7	4	0	0	0.01	0.9	24.0
3	0.5	1.3	1.1	83.0	0.93	448	9.6	200	88	10	2	0	0	0.01	1.0	44.0
2	0.3	1.3	1.1	82.7	0.92	448	9.5	219	79	12	9	0	0	0.01	1.0	9.0
1	0.1	1.5	0.9	83.0	0.91	446	9.1	212	83	10	6	0	0	0.00	1.8	13.5
c_{11} (Yuzhno-Donbasskaya #3)																
		1.9	3.1	81.4	0.70	436	5.6	249	56	15	29	0	0	0.00	0.5	1.9
c_{10} (Yuzhno-Donbasskaya #1)																
3	1.05	2.9	2.0	77.3	0.60	432	4.4	278	52	21	26	2	2	0.04	0.3	2.0
2	0.65	2.2	1.8	81.2	0.62	430	3.9	260	59	20	21	2	2	0.03	0.4	2.7
1	0.225	5.1	4.2	73.7	0.63	431	3.6	229	58	26	16	1	1	0.03	0.8	3.6

Grey shading indicates samples with more than 30% ash.

For chemical analysis, a representative portion of each sample was crushed to <250 μm to determine sulphur and total organic carbon (TOC) contents on a Leco CS-300 instrument. Ash yield and moisture content analyses followed standard procedures (Deutsches Institut für Normung, 1978, 1980). All ash and sulphur values are given as weight percents on a dry basis (db).

Rock Eval pyrolysis was performed in duplicate using a RockEval 2+ instrument (Espitalié et al., 1977; Peters, 1986). The amount of free hydrocarbons (S1) and the amount of hydrocarbons released from kerogen during gradual heating (S2) were determined. The latter was normalized to TOC to give the hydrogen index (HI = S2/TOC). As a maturation parameter, the temperature of maximum hydrocarbon generation (T_{max}, °C) was determined.

To characterize the molecular fraction, the powdered sediments were treated with chloroform at 60 °C for 45 min using a solvent extractor ASE200. The total extract obtained was fractionated by liquid chromatography on a silica column into saturates, aromatics and polars. Saturates and aromatics were analysed by gas chromatography-mass spectrometry in the laboratory of the UMR G2R (Unité de recherche Géologie et Gestion des ressources minérales et énergétiques, Nancy). The gas chromatograph was a Hewlett-Packard 5890 Series II and the detector a HP 5971 mass selective detector, operating in ''fullscan'' or SIM modes.

Inorganic geochemical analysis was performed using Instrumental Neutron Activation Analysis (INAA) and Inductively Coupled Plasma Emission Spectrometry (ICP-AES).

4. Results

4.1. Ash yield, inorganic geochemistry, and micropetrography

Ash yields, sulphur contents, and petrographic data are summarized in Table 1. The contents of major and some trace elements in coal ashes are listed in Table 2 together with typical trace element concentrations of ashes from bituminous coals after Krejci-Graf (1984).

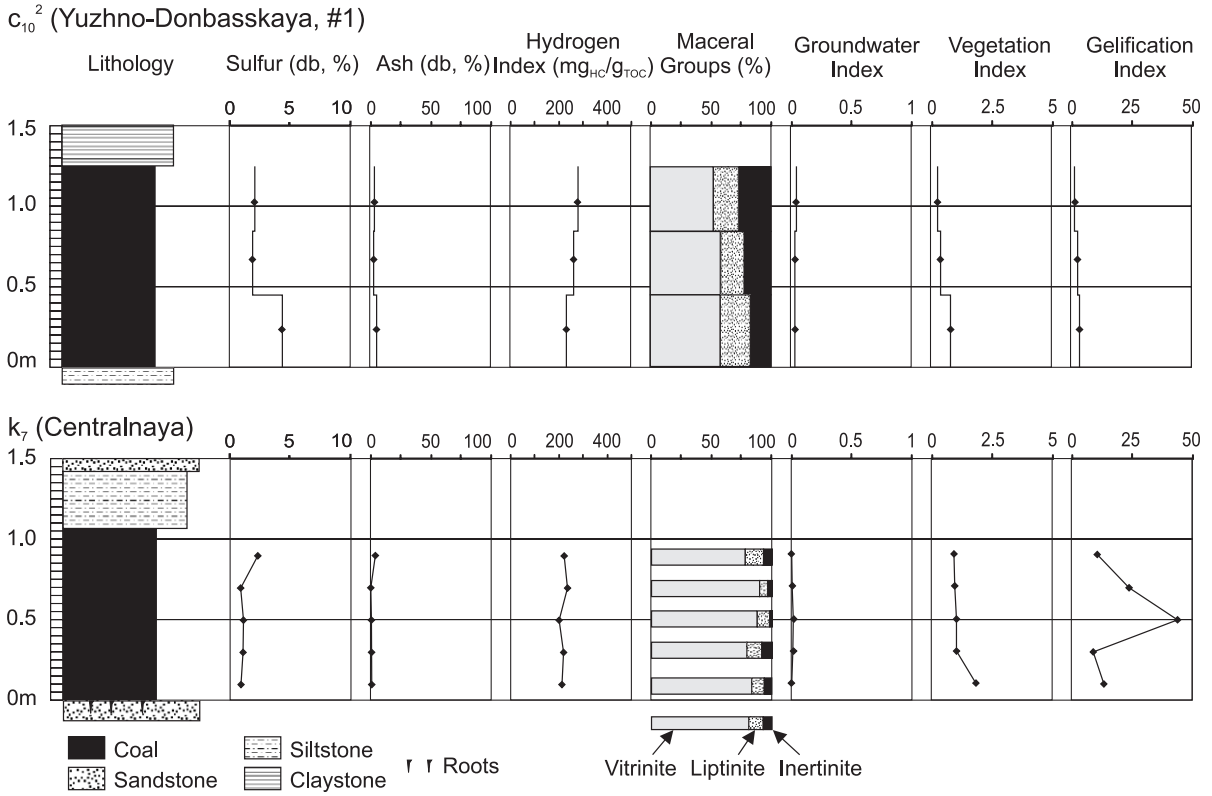

Fig. 3. Vertical distribution of sulphur, ash yield, hydrogen index, maceral groups (mineral free basis), and facies indicators in c_{10}^2 and k_7 seams.

Vertical variations within the seams are shown in Figs. 3, 4 and 7–11. The seams are described in a stratigraphic order from the oldest c^2_{10} to the youngest n_1 seam.

4.1.1. Seam c^2_{10} (Yuzhno-Donbasskaya #1)

The c^2_{10} seam in the studied section is 1.25 m thick. It overlies siltstone and is overlain by claystone (Fig. 3). The seam contains high volatile B/C bituminous coal (0.61% Rr) with an average ash yield of only 3.5%. Sulphur contents are moderately high (1.8–4.2%). The ash is dominated by Fe_2O_3 (Fig. 4), suggesting that pyrite is the most important mineral in the low-ash coal. Ni, As, and Cd contents are relatively high.

Considering all samples from the present study, there is a good correlation between iron contents of whole coals (<50% ash) and sulphur contents (r^2 = 0.87; n = 54) suggesting that pyrite is the main source for iron. However, Fe/S ratios are generally <0.813 indicating that pyrite is not the only sulphur source. Obviously, a significant part of the sulphur occurs within the organic matter (see also Bechtel et al., 2002).

Vitrinite contents range from 50% to 60%. Desmocollinite is the prevailing vitrinite maceral (Fig. 5a,b). Inertinite contents (mainly inertodetrinite, some pyrofusinite) are high and increase upwards from 16% to 26%. Liptinite percentages are in a similar range (20–26%). (Crassi)sporinite and liptodetrinite are the most abundant liptinite macerals. Macrospores occur in considerable amounts, and cutinite is rare. Because of abundant detrital macerals, the VI is generally low (0.5) with a maximum value of 0.8 in the lower part of

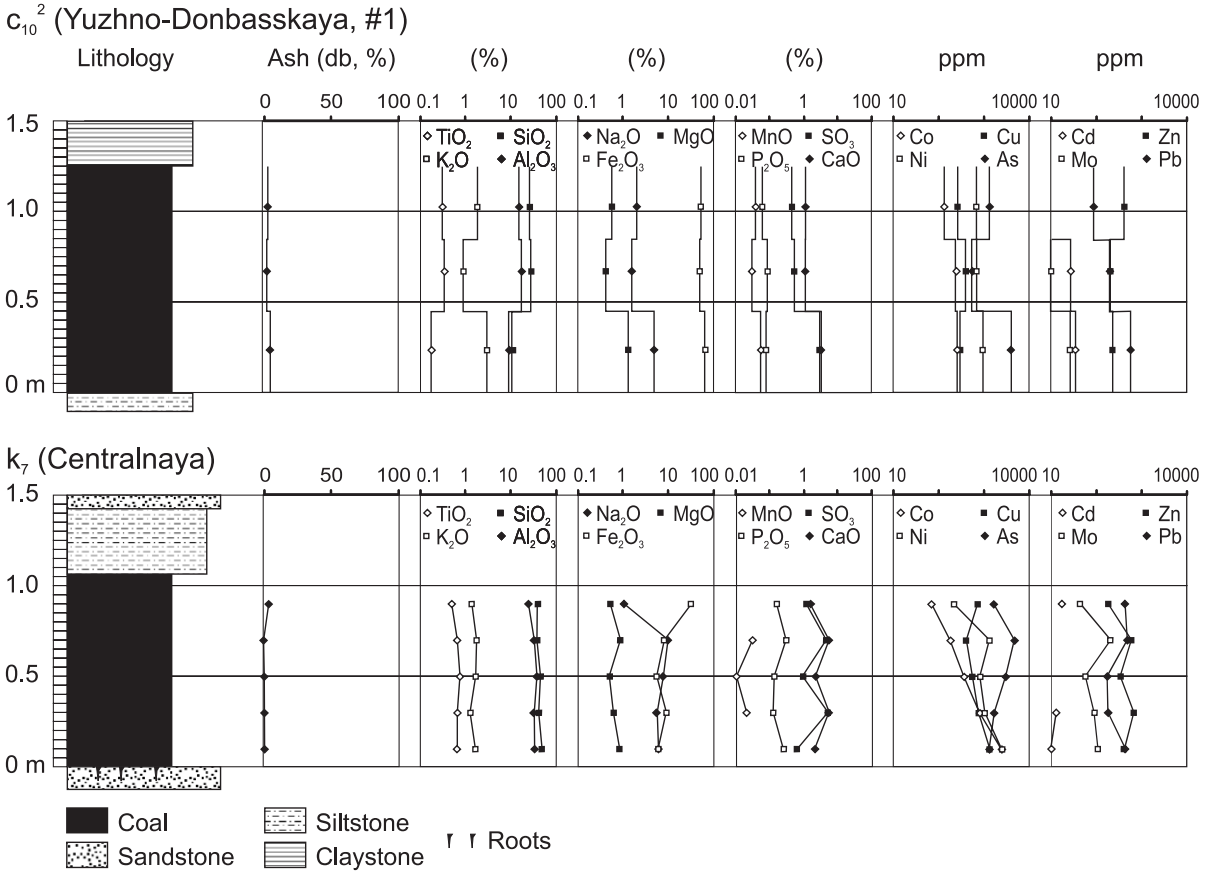

Fig. 4. Concentration of major and trace elements in c^2_{10} and k_7 seams.

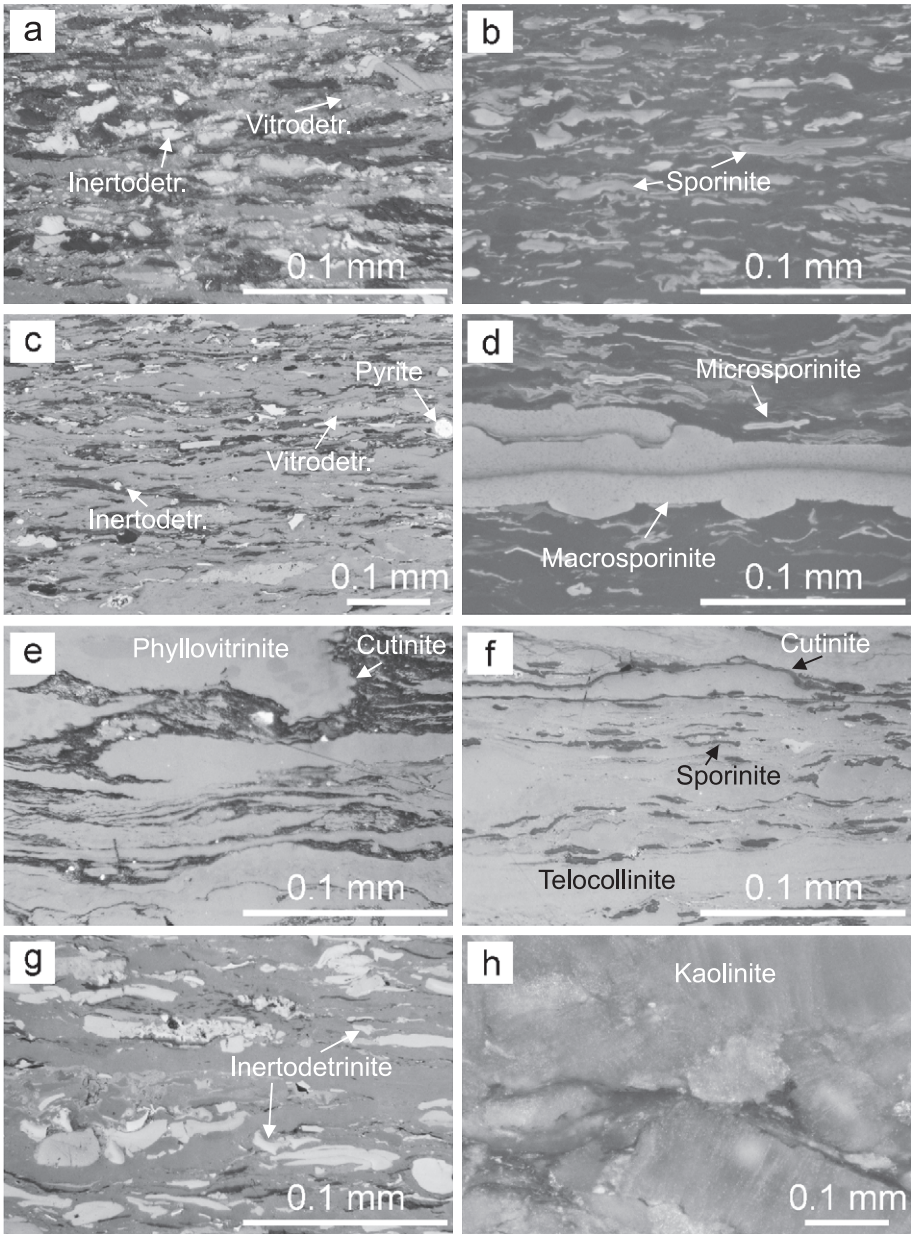

Fig. 5. Photomicrographs of coals from c^2_{l0}, l_1 and l_3 seams (oil immersion; incident white light except b, and d). (a) c^2_{l0} (Yuzhno-Donbasskaya, sample 1): Trimaceritic coal. (b) Same field as (a) (fluorescent mode): Sporinite is the main liptinite maceral. (c) l_1 (Novogrodovskaya, sample 1): liptinite-rich coal from the base of the seam. Vitrodetrinite and desmocollinite are the dominating vitrinite macerals. (d) l_1 (Dimitrova, sample 5; fluorescent mode): macrosporinite occurs in large quantities in the middle part of the seam. (e) l_3 (Almaznaya, sample 7): cross section through several leafs separated by shale. (f) l_3 (Almaznaya, sample 6): coal dominated by vitrodetrinite and thin layers of telocollinite. Sporinite and cutinite are present as well. (g) l_3 (Belozerskaya, sample 9): inertinite-rich coal. (h) l_3 (Belozerskaya, sample 4): kaolinite from the lower tuff layer.

the seam. GWI and GI are also low. The latter decreases upwards.

4.1.2. Seam c_{11} (Yuzhno-Donbasskaya #3)

Vitrinite reflectance of the studied section is 0.7% Rr (high volatile B bituminous). This 1.6-m-thick coal is low in ash yield (2%) but rich in sulphur (3%). Fe_2O_3 content is lower in the c_{11} seam than in the c^2_{10} seam (Table 2), demonstrating that despite high sulphur contents, pyrite is less abundant than in the c^2_{10} seam. Inertinite (29%) and lipinite (15%) percentages are high. GWI, VI, and GI are low and similar to those in the c^2_{10} seam (Table 1).

4.1.3. Seam k_7 (Centralnaya)

The studied seam section is about 1.1 m thick and overlies rooted sandstone (Fig. 3). The roof is formed by siltstone 35 cm thick and another sandstone 13.4 m thick. The k_7 seam is of high volatile A bituminous rank (0.92% Rr).

A shaly seam split occurs 20 cm below the top of the seam in the Dimitrova mine but is missing in the studied profile. The average ash yield in the Centralnaya section is only 1.9%. High percentages of SiO_2 and Al_2O_3 indicate that the ash is dominated by alumosilicates. Sulphur contents are moderate (1.2%) and reach a maximum (2.3%) near the top of the seam. Iron is abundant only in the uppermost sulphur-rich sample (Fig. 4).

The lower part of the seam is rich in Ni (2500 ppm) and Co (2400 ppm) and the contents in both elements decrease upwards (Fig. 4). As contents (1000–5000 ppm) are high within the entire seam. Concentrations of Pb and Zn are moderate, but in contrast to most other seams, Pb is less abundant than Zn.

Inertinite macerals are rare (5.6%) compared to other seams. In contrast, liptinite (predominantly tenuisporinite and liptodetrinite) content is relatively high (11%). Vitrinite percentages range from 78% to 89%. The VI decreases from the base towards the top of the seam. A very low GWI results from the virtual lack in detrital minerals. High GI values in the middle part of the seam reflect the very low inertinite contents.

4.1.4. Seam l_1 (Dimitrova, Novogrodovskaya #3, 13bis)

Fig. 6 illustrates a 40-km-long N–S section through the l_1 seam. Two tuff horizons occur within the seam. In the northern section the seam is split by fine-grained fluvial rocks (Uziyuk et al., 1972). The upper coal layer (l_1^{upper}) starts with coaly shale. The uppermost part of the seam is eroded along the southern section.

The l_1 seam is studied in profiles Dimitrova and Novogrodovskaya located near the section presented in Fig. 6, and in the 13bis mine northeast of Donetsk (Fig. 7; see inset in Fig. 6 for location of mines). Seam thickness is about 2 m in the western part and about 1 m in 13bis. The thin lower tuff, about 5 cm thick, is evident in all profiles. Claystone and coaly shale in the upper part of the Dimitrova and Novogrodovskaya profiles represent the fluvial seam split. The roof of the seam in the Dimitrova profile is formed by sandstone.

Ash yields are generally low (2–8%). Obviously, ash yields are significantly higher in samples containing tuff (Novogrodovskaya: kaolinite-rich sample 1) and samples from fluvial seam splits. The upper part of the seam (l_1^{upper}) in Dimitrova contains low-ash coal (c. 10% ash) but consists of coaly shale (60% ash) in the Novogrodovskaya section. Minor authigenic quartz occurs below the tuff in the 13bis section. Sulphur contents of low-ash coals (< 10% ash) range from 3% to 7.5%. The highest values occur at the base and at the top of the seam in the Dimitrova section. Sulphur contents of high-ash coals, coaly shales, and claystones are negatively correlated with ash yields ($r^2 = 0.86$; $n = 7$).

The Dimitrova (0.74% Rr) and Novogrodovskaya (0.72% Rr) profiles contain high volatile bituminous coal, whereas medium volatile bituminous coal (1.39% Rr) occurs in location 13bis. Because of the advanced rank, liptinites are not observable in the 13bis section. The rank difference between the sections shows the general eastward increase in maturity in the western Donets Basin.

Inorganic geochemical data are available from the Dimitrova section (Fig. 8). There, the shaly seam split is characterized by high percentages of SiO_2 (60%), Al_2O_3 (30%), and K_2O (4%). Similar chemical signatures of samples at 0.7 and 1.7 m (samples 4, 8; Table 2) suggest that the mineral matter in these samples is dominated by detrital minerals. In contrast, the ash of low-ash coals from the base of the seam (0–0.5 m; samples 1–3) is dominated by Fe_2O_3 (55–80%) suggesting that pyrite is the main mineral present. Samples below and above the seam split are mixtures between both end member types.

Table 2
Concentration of elements in ash of Donets Basin samples

Sample	Ash	SiO_2	$Al2O_3$	TiO_2	Fe_2O_3	MgO	CaO	MnO	Na_2O	SO_3	P_2O_5	K_2O	Pb	Zn	Cd	Cu	Ni	Co	As	Mo
	%						%						ppm							
Typical concentrations after Krejci-Graf (1984):													**10-800**	**10-2000**	**5-10**	**10-1000**	**10-1000**	**10-300**	**50-1000**	**1-500**
n_1 (Butovskaya)																				
5	4.3	11.8	12.9	0.3	49.6	1.3	9.9	0.05	0.8	12.6	0.12	0.2	139	146	<4	263	368	250	1276	107
4	11.6	44.5	30.6	0.6	8.4	1.8	4.5	0.02	1.1	4.4	0.43	3.4	178	58	<4	261	82	<4	143	<5
3	2.0	19.3	19.8	0.4	27.9	2.3	13.2	0.06	2.2	13.2	0.17	0.9	111	105	11	326	400	178	777	57
2	6.9	41.6	34.2	0.7	10.3	0.9	4.3	0.02	1.4	2.2	2.88	1.2	534	154	<4	488	138	63	154	28
1	9.5	46.9	34.2	0.7	10.0	1.4	1.0	0.01	1.2	0.4	0.30	3.7	337	146	26	506	1319	91	216	39
m_5 (Almaznaya)																				
5	1.4	49.2	34.6	0.7	8.6	0.9	2.5	0.01	1.2	0.2	0.27	1.5	1267	1432	15	545	510	242	789	154
4	14.2	29.6	20.6	0.4	46.2	0.3	0.6	<0.01	0.4	0.2	0.12	1.2	376	58	17	169	180	15	562	58
3	2.5	27.5	21.2	0.4	45.3	0.7	2.1	0.01	0.8	0.2	0.22	1.1	1762	696	31	286	579	200	1272	131
m_3 (Bazhanova)																				
10	36.1	62.5	20.4	0.4	10.3	1.0	0.5	0.01	1.4	0.3	0.06	2.8	257	150	<4	159	98	21	175	<5
8	2.8	40.1	14.4	0.3	40.5	0.4	1.5	0.04	1.4	0.5	0.14	0.7	238	492	12	263	164	35	886	41
7	2.9	31.3	5.4	0.1	58.3	0.4	2.0	0.02	1.3	0.4	0.07	0.2	812	804	20	131	52	<4	4376	23
6	3.1	33.4	4.2	0.1	57.8	0.3	1.3	0.02	1.6	0.9	0.05	0.3	257	210	31	81	45	<4	804	13
5	47.2	92.5	0.4	<0.01	5.2	<0.01	0.7	<0.01	0.1	0.6	<0.03	0.2	<25	38	<4	21	19	<4	105	<5
4	8.7	24.5	7.0	0.1	57.0	0.9	5.0	0.03	0.5	3.9	0.08	0.5	<25	289	14	39	45	31	1058	<5
3	0.9	36.4	28.7	0.6	11.8	1.6	7.2	0.02	5.9	5.9	0.16	1.3	459	242	<4	1087	451	176	6742	66
2	8.6	13.8	4.8	0.1	61.5	0.8	9.1	0.05	2.4	6.1	<0.03	1.5	314	310	39	114	82	<4	1443	<5
1	42.6	63.8	19.7	0.4	9.3	1.0	0.6	0.01	1.8	0.3	0.06	2.8	<25	178	<4	154	82	21	386	<5
m_2 (Belitskaya)																				
7	20.0	36.1	23.4	0.5	23.0	1.0	6.5	0.04	0.5	6.1	0.09	2.3	178	18	16	173	96	21	224	13
6	6.7	13.0	4.8	0.1	29.0	0.3	23.9	0.13	0.2	27.6	0.07	0.4	257	138	<4	214	73	37	781	11
5	4.7	28.3	13.0	0.3	53.0	0.6	1.8	0.03	0.6	0.9	0.09	1.3	534	369	33	289	255	51	1136	34
4	89.1	60.2	29.1	0.6	3.2	1.7	0.5	0.01	0.5	0.2	0.07	4.0	178	86	<4	49	73	14	<10	<5
3	12.0	48.1	31.0	0.6	12.0	1.3	1.7	0.02	0.6	1.2	0.11	3.1	297	218	<4	225	269	50	297	22
2	17.6	28.4	9.2	0.2	38.9	0.6	11.4	0.08	0.7	8.4	0.08	1.7	175	204	6	201	90	19	138	18
1	21.2	39.0	22.1	0.4	33.5	1.1	0.5	0.01	0.4	0.3	0.06	2.6	99	130	<4	122	281	65	315	14
l_3 (Almaznaya)																				
11	9.6	51.3	6.9	0.1	5.2	6.4	14.1	0.14	0.4	15.2	0.18	0.3	238	26	<4	85	77	60	4904	68
10	1.4	49.6	32.1	0.6	2.0	1.4	5.7	0.04	4.5	2.6	0.31	0.6	1544	863	<4	419	320	98	7999	66
9	2.6	30.9	22.3	0.5	41.5	0.7	1.6	0.02	1.4	0.2	0.11	0.9	633	545	<4	483	663	99	2319	64
8	1.8	40.8	30.8	0.6	21.0	0.5	2.1	0.01	2.0	0.2	0.88	0.6	342	529	<4	924	793	340	2406	83
7	35.6	55.0	34.0	0.7	2.3	1.4	0.5	0.01	1.0	0.1	0.10	4.5	238	130	11	171	82	17	305	<5
6	5.1	50.0	32.5	0.7	10.7	0.9	0.8	<0.01	0.8	0.1	0.12	3.0	317	473	<4	539	532	146	983	47
l_3 (Belozerskaya)																				
12	7.4	52.2	6.1	0.1	19.4	0.8	9.3	0.07	0.5	10.7	0.06	0.2	218	186	19	110	68	31	606	55
10	3.4	43.3	15.1	0.3	35.9	0.5	2.0	0.03	1.1	1.3	0.09	0.2	<25	<4	15	294	162	54	854	18
9	9.7	7.7	5.4	0.1	30.9	0.6	24.5	0.16	1.3	28.4	<0.03	0.6	<25	139	<4	138	69	7	1798	15
8	67.5	59.9	28.7	0.6	3.8	1.3	0.4	<0.01	0.9	0.0	0.06	4.0	198	54	<4	85	49	<4	<10	<5
7	24.3	52.3	32.3	0.7	7.5	1.3	0.5	<0.01	1.0	0.1	0.09	3.9	574	130	<4	247	134	71	<10	<5
6	85.0	57.4	31.6	0.6	2.9	1.4	0.4	<0.01	1.0	0.0	0.07	4.2	337	82	<4	80	50	45	<10	<5
5	4.9	22.9	15.8	0.3	55.2	0.4	0.7	<0.01	1.0	0.1	0.06	1.1	257	234	20	211	232	13	256	25
4	63.5	52.8	42.3	0.9	1.2	0.3	0.6	<0.01	0.7	0.0	0.19	0.6	297	130	<4	47	12	<4	<10	<5
3	11.6	49.5	33.1	0.7	7.6	1.2	1.5	0.01	0.9	1.4	0.14	3.7	198	134	<4	247	91	24	61	16
2	1.5	41.0	31.3	0.6	15.9	0.5	3.2	0.02	3.0	2.5	0.13	1.4	336	375	21	861	657	315	481	191
1	3.4	33.1	22.3	0.5	38.3	0.5	1.4	<0.01	1.2	0.8	0.09	1.4	693	273	11	512	1038	673	726	96

Table 2 (*continued*)

Sample	Ash	SiO_2	$Al2O_3$	TiO_2	Fe_2O_3	MgO	CaO	MnO	Na_2O	SO_3	P_2O_5	K_2O	Pb	Zn	Cd	Cu	Ni	Co	As	Mo
	%						%						ppm							
l_1 (Dimitrova)																				
9	9.3	30.0	20.0	0.4	44.9	0.7	0.9	0.02	0.6	0.3	0.14	1.7	455	146	17	354	269	73	303	16
8	10.0	45.9	30.6	0.6	16.0	1.1	0.9	0.01	0.7	0.5	0.16	3.2	218	154	16	411	307	67	114	24
7	90.6	59.5	31.2	0.6	2.1	1.3	0.4	<0.01	0.7	0.1	0.07	4.2	198	62	<4	109	68	<4	<10	<5
6	2.3	29.1	22.3	0.5	39.7	0.6	2.7	0.03	2.4	0.5	0.24	1.5	304	324	13	911	434	54	579	128
5	1.5	22.4	17.0	0.3	49.6	0.7	3.8	0.05	1.8	2.3	0.12	1.5	174	321	30	547	500	39	1305	139
4	13.6	57.5	30.2	0.6	5.6	1.1	0.8	<0.01	0.7	0.3	0.11	2.8	297	<4	13	845	101	47	122	35
3	4.1	20.2	14.9	0.3	60.2	0.4	1.6	0.02	1.2	0.5	0.10	0.9	574	146	19	495	241	27	1154	123
2	3.3	21.9	14.0	0.3	57.6	0.5	2.0	0.03	1.0	1.3	0.13	1.0	659	322	19	332	165	37	603	159
1	8.3	8.3	5.5	0.1	78.5	0.2	1.4	0.01	2.2	0.8	0.06	2.9	<25	312	29	240	536	23	380	118
k_7 (Centralnaya)																				
5	4.4	38.0	24.4	0.5	31.0	0.5	1.5	<0.01	1.0	1.1	0.15	1.4	428	178	17	728	214	69	1674	43
4	0.7	37.0	32.5	0.7	8.0	0.9	5.3	0.03	9.7	4.5	0.29	1.8	479	592	<4	414	1322	179	4733	206
3	1.3	44.4	37.0	0.7	5.4	0.5	2.1	0.01	7.7	0.9	0.13	1.7	172	334	<4	559	817	360	3007	56
2	1.3	40.6	32.7	0.7	8.8	0.6	5.3	0.02	5.6	4.9	0.12	1.3	179	669	13	758	1050	791	1696	88
1	1.5	48.6	33.1	0.7	5.9	0.8	2.1	<0.01	5.9	0.6	0.24	1.6	436	416	10	1337	2466	2386	1307	106
c_{11} (Yuzhno-Donbasskaya #3)																				
	1.9	39.5	30.4	0.6	22.3	0.8	1.3	0.03	2.5	1.1	0.13	0.9	282	309	<4	194	966	84	643	7
c_{10}^2 (Yuzhno-Donbasskaya #1)																				
3	2.9	26.4	15.3	0.3	51.6	0.6	1.1	0.04	2.0	0.5	0.06	1.9	89	417	<4	258	683	132	1335	<5
2	2.2	28.1	17.7	0.4	48.8	0.4	1.0	0.03	1.5	0.6	0.09	0.9	203	199	27	402	682	238	558	10
1	5.1	10.9	9.1	0.2	64.6	1.3	2.9	0.06	4.7	3.2	0.08	3.0	581	239	36	295	956	263	4087	26

High-ash coals and seam splits are indicated by grey shading. Bold numbers denote typical values of trace elements of ashes from bituminous coals according to Krejci-Graf (1984).

In general, the ash from low-ash coals contains higher percentages of trace elements than that of mineral matter-rich coal. Co contents are moderate (20–75 ppm) but show a distinct upward increasing trend. Moderate As contents (300–1300 ppm) are negatively correlated with ash yields ($r^2 = 0.67$; $n = 9$).

Vitrinite is the dominant maceral group in all sections. The coal beneath the lower tuff in the Novogrodovskaya and Dimitrova sections is rich in liptinite (mainly sporinite; Fig. 5c) and inertinite. In contrast to the Novogrodovskaya section, degradofusinite is more abundant than pyrofusinite in the Dimitrova section. Relatively high contents in liptinite (including macrosporinite; Fig. 5d) and inertinite also occur in the middle part of the l_1 seam. Coaly shales in the Novogrodovskaya section are rich in vitrinite, whereas the l_1^{upper} seam in the Dimitrova section contains abundant inertinite (20–25%). VI is about 1 in most samples. The GWI is slightly raised only in the middle part of the Dimitrova section and in the lowermost sample from the Novogrodovskaya profile. GI values reach maxima about 0.5 m above the floor of the seam. Sporinite rich sapropelic coal is indicated in the cross section shown in Fig. 6. However, no sapropelic coals were encountered in the studied profiles.

4.1.5. Seam l_3 (Almaznaya, Belozerskaya)

A cross section along the l_3 seam, which is one of the thickest seams in the Donets Basin, is presented in Fig. 6. Seam thickness reaches 2.3 m in the Belozerskaya mine but is <0.4 m between the illustrated segments. Thickness variations are at least partly due to erosion, which removed the entire seam in the Novogrodovskaya mine and the upper part of the seam along the southern transect shown in Fig. 6. The l_3 seam contains several partings including two tuff layers 5 and 15 cm thick. The roof of the seam is formed by claystone.

The rank of coal from the Almaznaya and Belozerskaya mines is high volatile A bituminous (0.80–0.90 % Rr). The seam overlies rooted claystone in both sections (Fig. 9). Ash yields are generally low but often increase in samples near seam splits. Shaly coal occurs between the lowermost seam split and the lower tuff in the Almaznaya section. The chemical

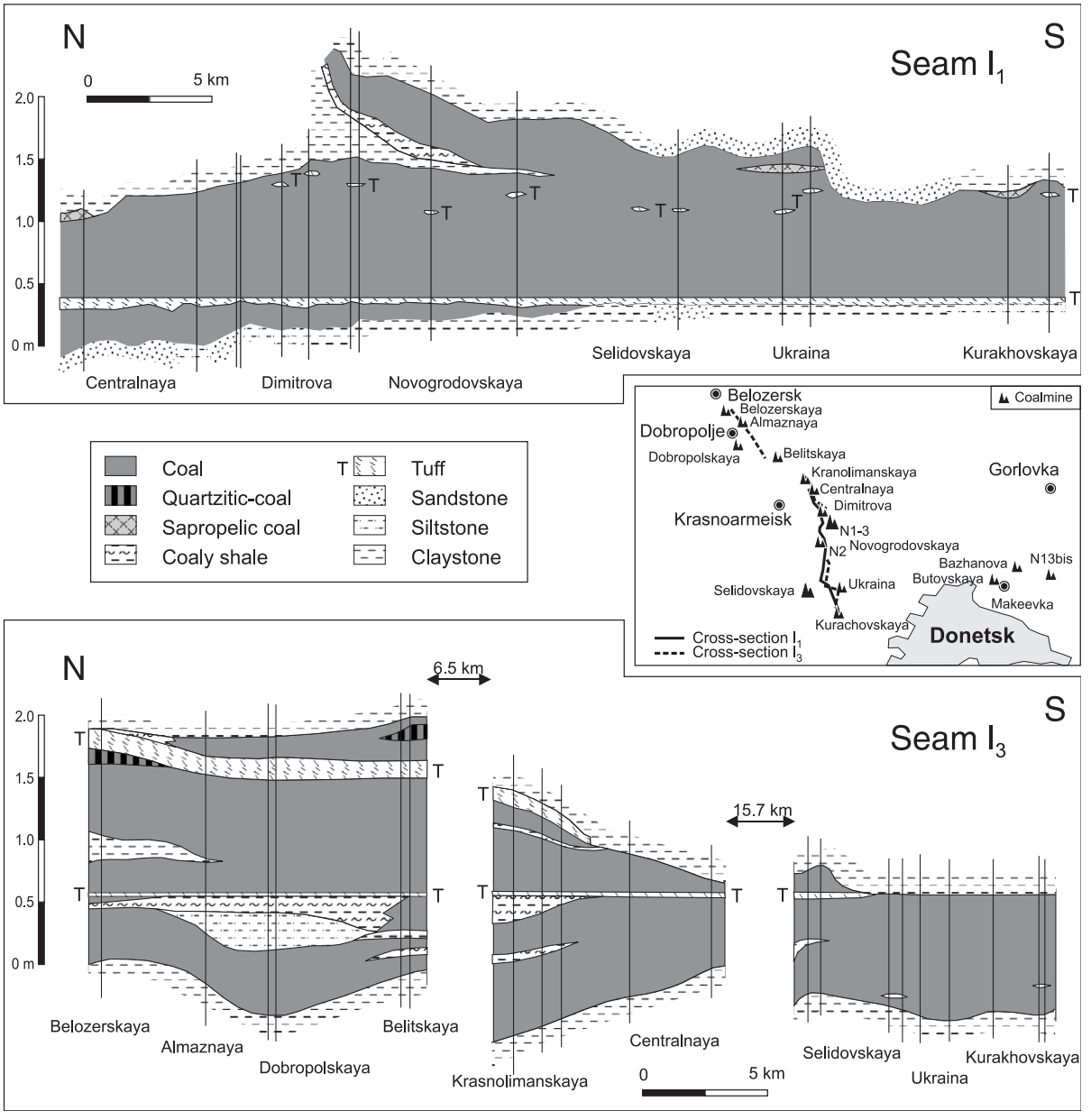

Fig. 6. Lithostratigraphic profiles along the l_1 and l_3 seams in the western Donets Basin. Tuff layers are used for correlation (after Uziyuk et al., 1972). Quartzitic coal: coal with abundant authigenic quartz. The position of the profiles is shown in the inset.

signature of detrital seam splits and of shaly coal is similar to that of the l_1 seam split. The chemical signature of the lower tuff layer in the Belozerskaya section (sample 4; Table 2) differs significantly showing higher Al_2O_3 content (42%), a slightly lower SiO_2 content (53%) and significantly lower percentages of K_2O (0.6%) and MgO (0.3%; Fig. 8). This composition suggests kaolinite as the predominant mineral and agrees with analyses from other tuffs in the Donets Basin (Zaritsky, 1972). Ash yields of the uppermost sample in both sections are slightly increased (9.6% and 7.4%, respectively). Microscopic examination

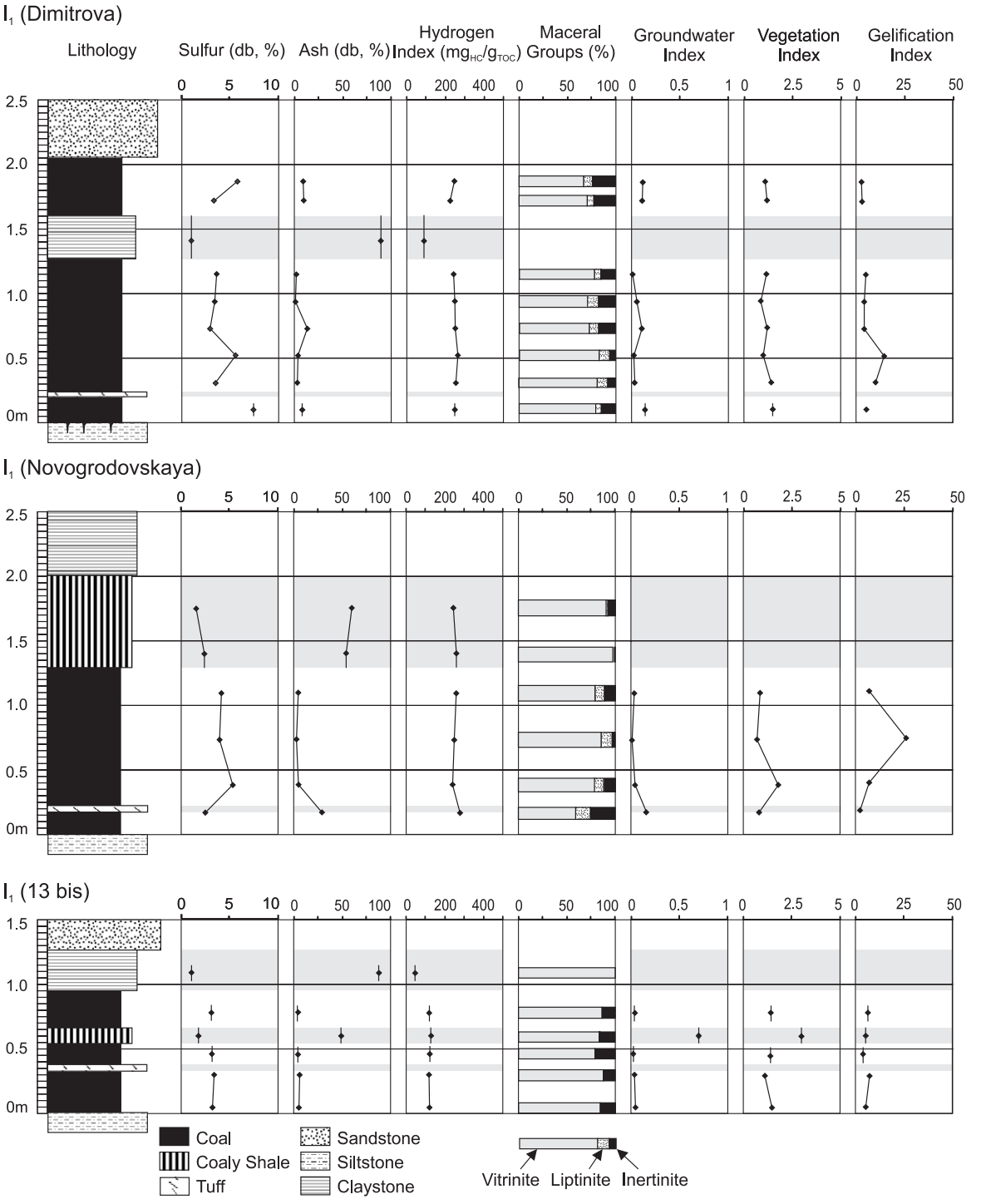

Fig. 7. Vertical distribution of sulphur, ash yield, hydrogen index, maceral groups (mineral free), and facies indicators in seam l_1 (Dimitrova, Novogrodovskaya, 13bis mines).

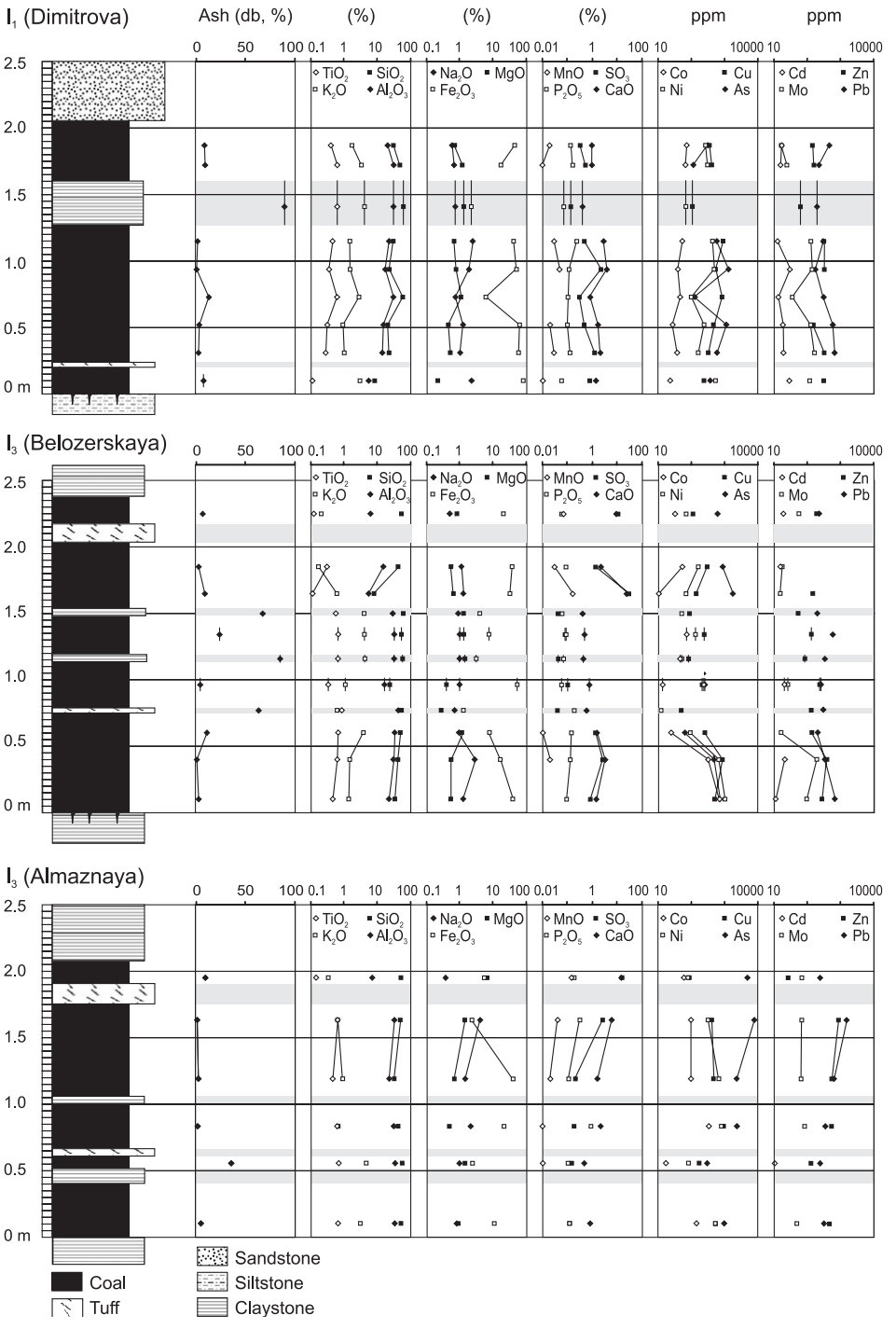

Fig. 8. Concentration of major and trace elements in l_1 and l_3 seams.

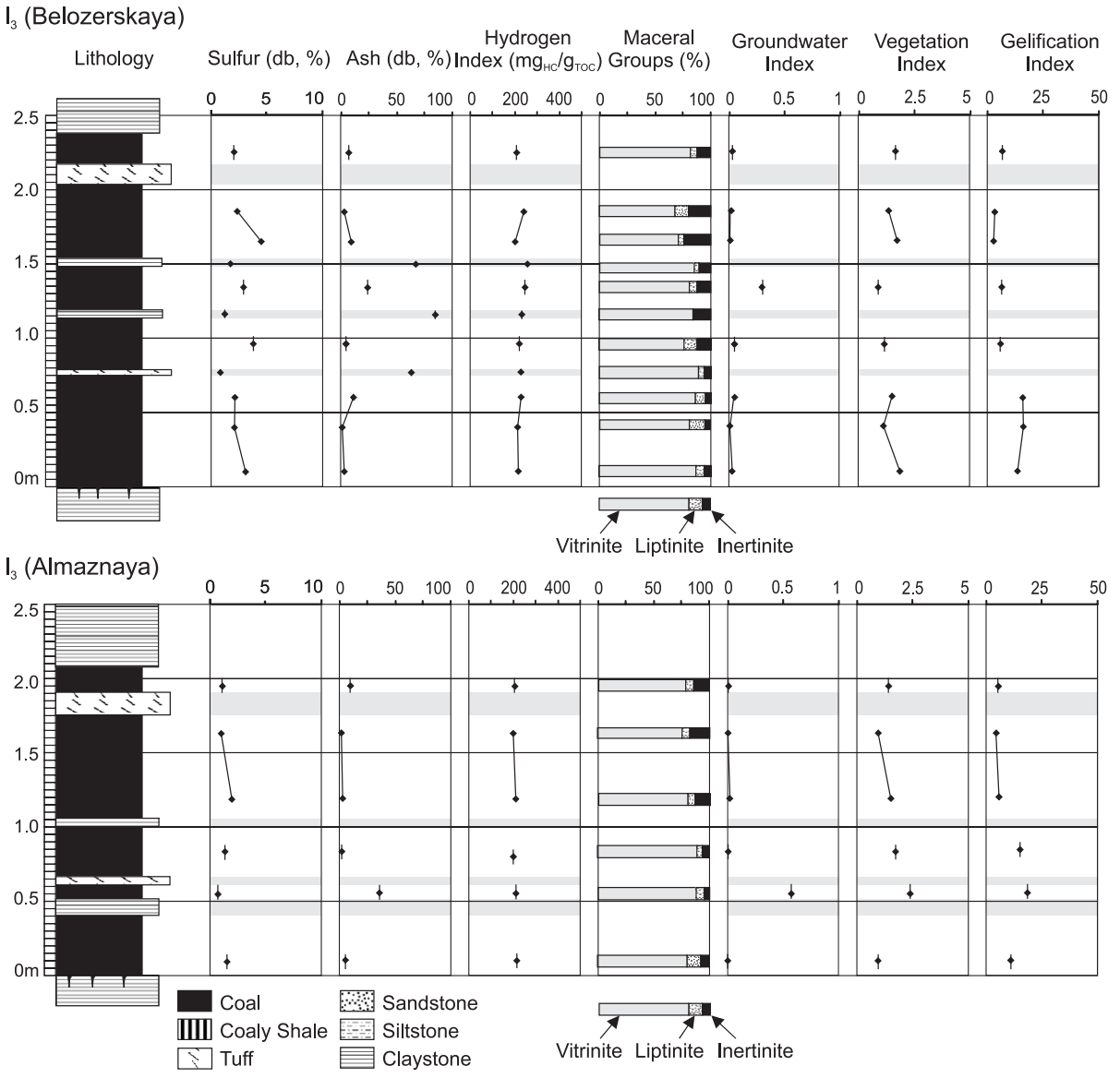

Fig. 9. Vertical distribution of sulphur, ash yield, hydrogen index, maceral groups (mineral free), and facies indicators in seam l_3 (Belozerskaya, Almaznaya mines).

shows that this is due to the presence of authigenic quartz and epigenetic carbonate. The presence of authigenic quartz is reflected by unusually high SiO_2/Al_2O_3 ratios (2.9–7.5), whereas high calcium and magnesium contents (6.4% MgO) in the uppermost Almaznaya section (Fig. 8) indicate the presence of manganese-rich calcite or dolomite. The sulphur content in low-ash coal is significantly higher in the Belozerskaya section (2.8%) than in the Almaznaya section (1.3%).

As contents are very high in ash from the upper part of the Almaznaya section (2000–8000 ppm). Co contents reach maxima near the base of the seam and are especially high in the Belozerskaya section (673 ppm).

The ash-rich sample below the lower tuff in the Almaznaya section is rich in leaves (Fig. 5e). The

lowermost sample contains abundant spores (Fig. 5f). Inertinite contents are generally low in the lower half of the seam but reach maxima, with up to 24%, below the upper tuff (Fig. 5g). High inertinite contents are also observed above the upper tuff (<14%). The GI shows parallel trends in both sections with maxima below the lower tuff and minima below the upper tuff (Fig. 9). The VI of both sections is relatively high and ranges from 1 to 2. The GWI is very low. Relatively high values are restricted to ash-rich samples. Sample 4 from the Belozerskaya section represents the lower kaolinitic tuff (Fig. 5h).

4.1.6. Seam m_2 (Belitskaya)

The m_2 seam in the Belitskaya region is about 1 m thick. The floor and roof of the seam are formed by siltstone. A shaly parting 12 cm thick separates a high-ash lower part from a low-ash upper part (ca. 5%; Fig. 10). Ash yield increases to 20% at the top of the seam. The average sulphur content of coal is 5.2%. These are the highest sulphur values of all studied seams. Sulphur maxima occur near the base of the seam (>8%). A slight increase in sulphur is also observed below its roof. Very high pyrite contents relate to high concentrations in iron.

The chemical signature of the shaly seam split corresponds to that of other detrital seam partings in the Donets Basin. The coal ash above and below the seam split is relatively rich in CaO (Fig. 11). SiO_2/Al_2O_3 ratios are higher than in most other seams. Heavy metal contents are within the range of typical concentrations of these elements in ash from bituminous coals (Table 2). Only sample 5 is enriched in Cd and As.

Average vitrinite reflectance (0.68% Rr) classifies the coal as high volatile B bituminous. Vitrinite reflectance decreases near the top of the seam to 0.64% Rr.

Liptinite percentages are typically in the order of 6% to 7%. Only the uppermost ash-rich coal contains 17% liptinites, with tenuisporinite as the most abundant maceral. Average inertinite content is about 10%. VI values are generally low (average VI about 1) and VI values decrease upwards in the upper part of the seam. The GWI reaches maxima (0.2) near the base and the top of the seam. GI values are high in the lower portion of the seam and low with an upward decreasing trend in its upper part.

4.1.7. Seam m_3 (Bazhanova)

The seam section is 1.55 m thick, which is slightly lower than the average thickness in the Bazhanova mine (1.65 m; Triplett et al., 2001). The seam overlies siltstone, the roof is formed by claystone. A 6-cm tuff layer with coarse kaolinite crystals splits the seam a few centimetres below the top (Fig. 10). Rank of the studied section is medium volatile bituminous (1.18% Rr).

Ash yields are generally low (<5%) but significantly increased in the lowermost part of the seam and above the tuff layer. The mineral matter in the ash-rich coal includes thin layers with large biotite crystals, feldspar, and quartz phenocrysts (Fig. 12a). Samples with tuffogenous minerals contain more than 60% SiO_2 and about 20% Al_2O_3. Ash from the lower part of the seam contains CaO in significant amounts (Fig. 11).

Authigenic quartz causes high ash yields in the middle part of the seam (sample 5; Fig. 12b) and results in a very high SiO_2 content (92.5%; Fig. 11). Quartz crystals reach diameters >0.1 mm and are also present in minor amounts in sample 6. Quartz also fills cell lumens of fusinite (Fig. 12c). Migrated bitumen with a strong orange fluorescence colour is sometimes associated with the authigenic quartz and forms thick granular or fibrous coatings. Framboidal pyrite occurs within the organic matter, whereas idiomorphic pyrite often forms the center of quartz crystals. Migrated bitumen also occurs in other samples and is especially abundant in sample 2, where it fills cracks, predominantly in inertinite.

Sulphur values ranges from 0.5% to 7.5% and are positively correlated with ash yields in low-ash coals (<10% ash; $r^2 = 0.91$; $n = 6$). Average sulphur content is about 4%. High iron concentrations are consistent with abundant pyrite. As contents of >4000 ppm occur in ash from two low-ash coal samples.

Because of advanced rank, primary liptinites are not visible in the studied section. The ash-rich samples near the top and the base of the seam contain exclusively vitrinite. Inertinite percentages in low-ash coals ranges from 9% to 22%. Inertodetrinite and degradofusinite occur in high proportions. Pyrofusinite is abundant only in sample 5 (7%). With the exception of the base and the top of the seam, the GWI is very low (<0.1). The VI shows a wide scatter. GI is very high in the uppermost and lowermost samples but low in the bulk of the seam.

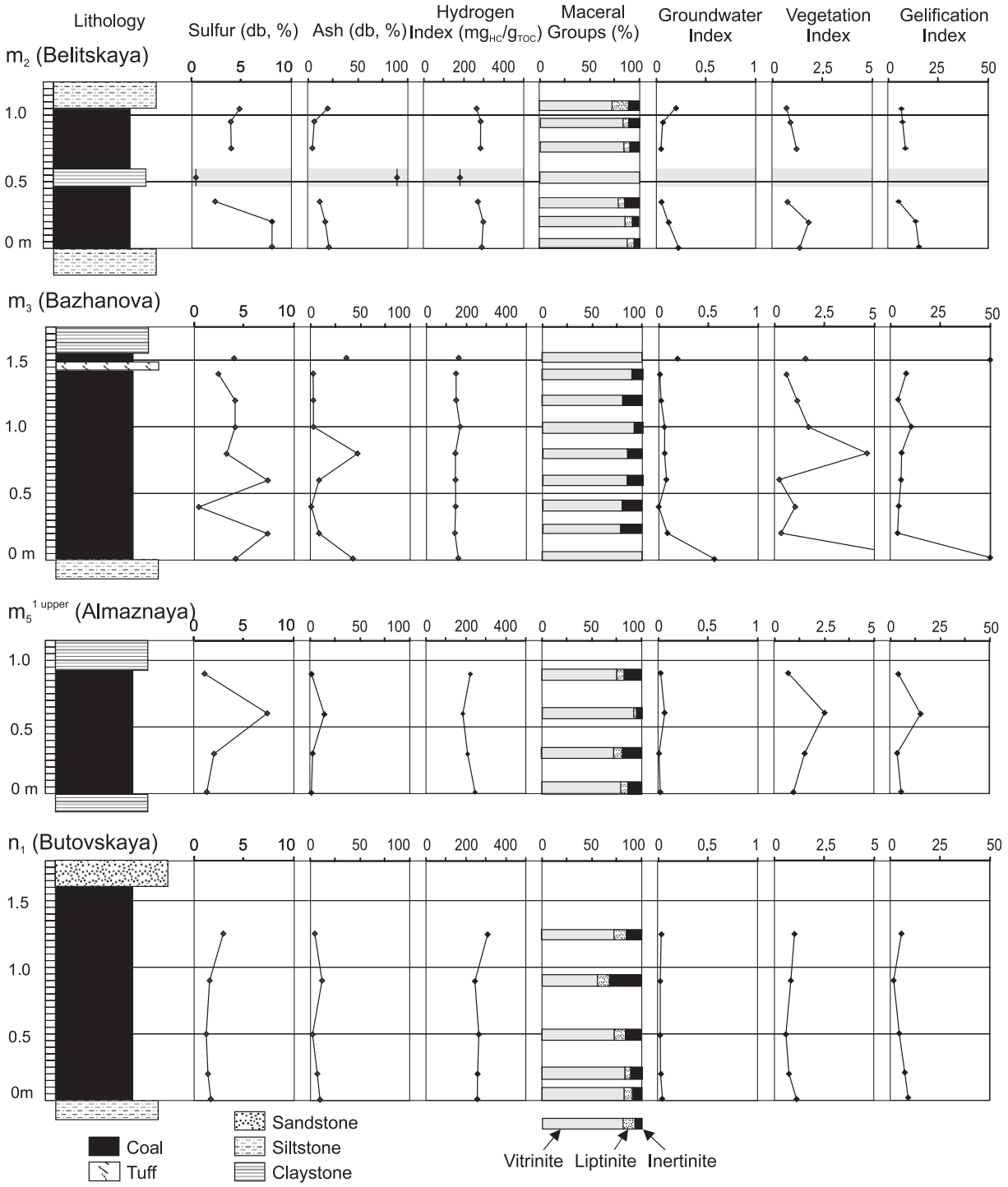

Fig. 10. Vertical distribution of sulphur, ash yield, hydrogen index, maceral groups (mineral free), and facies indicators in m_2, m_3, $m_5^{1\ upper}$, and n_1 seams.

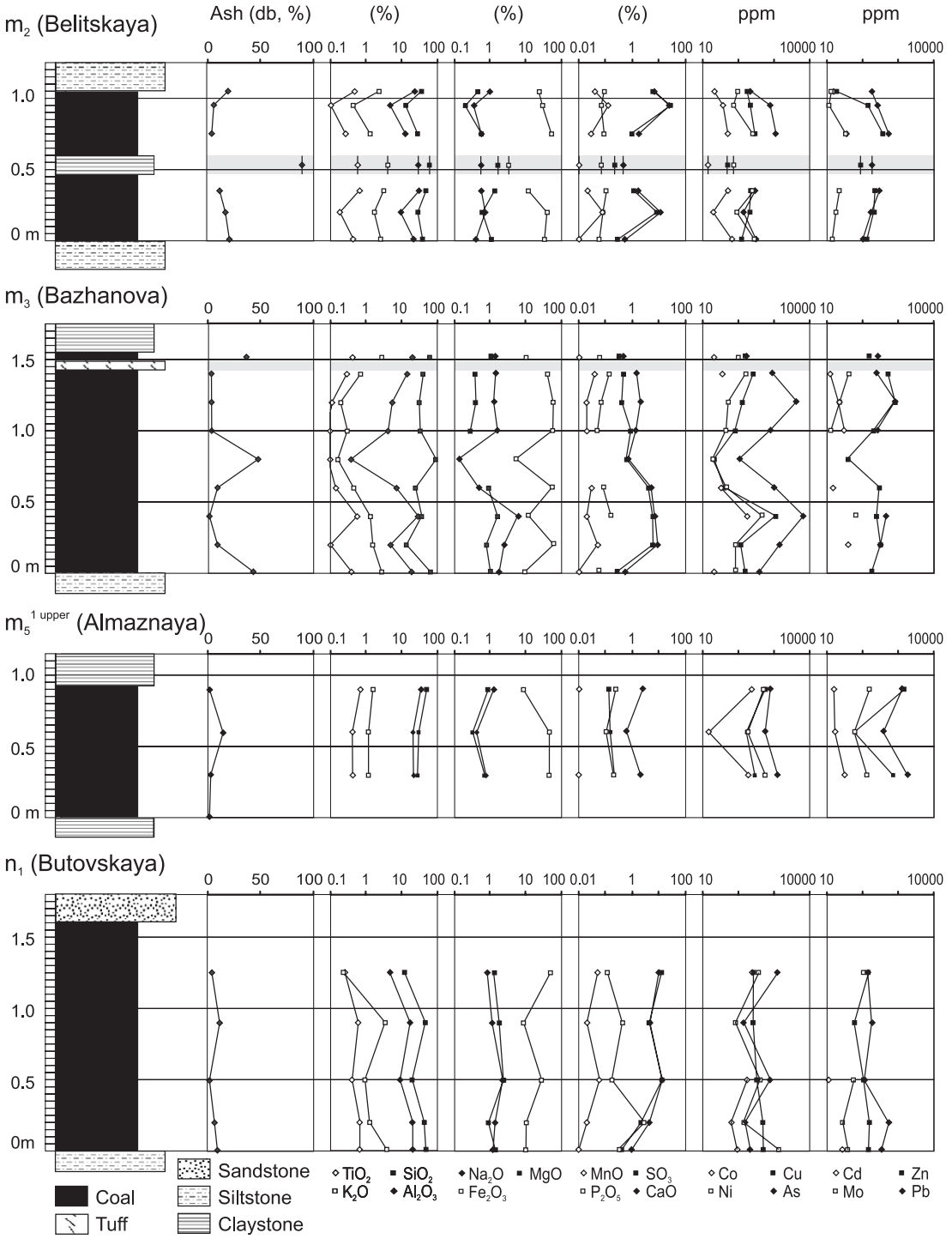

Fig. 11. Concentration of major and trace elements in m_2, m_3, $m_5^{1\ upper}$, and n_1 seams.

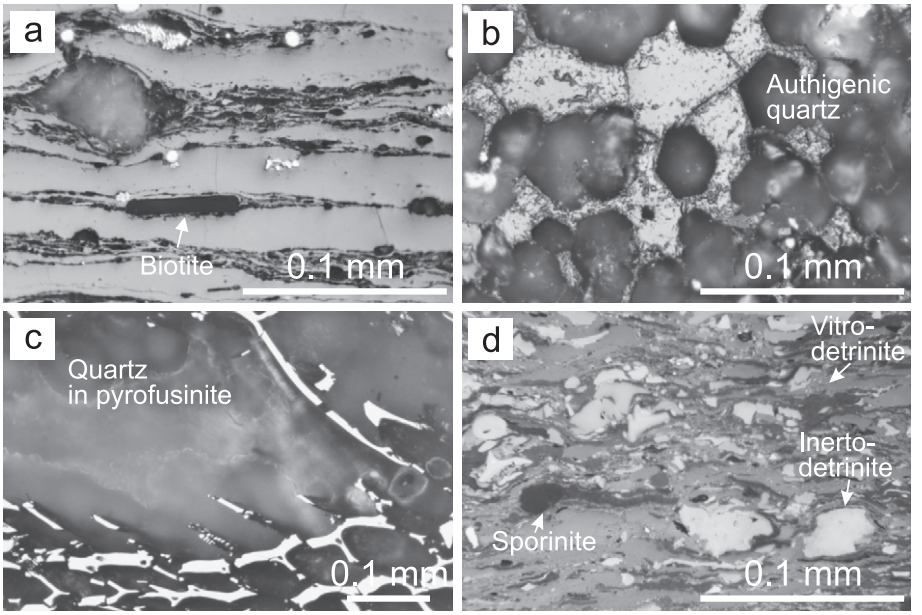

Fig. 12. Photomicrographs of coals from m_3, and n_1 seams (oil immersion; incident white light). (a) m_3 (Bazhanova, sample 10): volcanogenic minerals within vitrinite-rich coal. (b) m_3 (Bazhanova, sample 5): authigenic quartz. (c) m_3 (Bazhanova, sample 5): quartz in fusinite. (d) n_1 (Butovskaya, sample 4): trimacerite.

4.1.8. Seam $m_5^{1\ upper}$ (Almaznaya)

The $m_5^{1\ upper}$ seam in the Almaznaya section contains high volatile bituminous B coal (0.73% Rr) and is about 1 m thick. Claystone underlies and overlies the seam (Fig. 10). Average ash yield is 5%. Thin layers with kaolinite are present in the upper part of the seam. Sulphur contents generally range from 1% to 2% but are very high (7.3%) in sample 4, which contains massive epigenetic pyrite filling cell lumens in fusinite. Although percentages are only moderate, the $m_5^{1\ upper}$ seam is amongst the richest seams in Pb, Zn, Cd, and Mo (Table 2). Inertinite contents range from 6% to 19% and correlate with liptinite ($r^2 = 0.94$; $n = 4$). Average VI is about 1.5, indicating a high proportion of decay resistant plants. GWI (~ 0.03) and GI (< 10) are low.

4.1.9. Seam n_1 (Butovskaya)

The n_1 seam reaches its largest thickness (up to 2.4 m) in the Donetsk-Makeevka region. A 1.6-m-thick section was sampled in the Butovskaya mine. Here, the seam overlies siltstone and is overlain by sandstone (Fig. 10).

Ash yield is generally low (7%). Samples with ash yields above 5% are dominated by SiO_2 and Al_2O_3, indicating a predominance of clay minerals. Ca and Fe concentrations are high in low-ash coals. The sulphur content is moderate but increases in the uppermost sample to 2.9%. Pb, Zn, and Cu contents are moderate and the concentrations of all three elements decrease upwards (Fig. 11).

Vitrinite reflectance decreases upwards from 0.85% to 0.63% Rr. A negative correlation with the amount of free hydrocarbons (RockEval peak S1; $r^2 = 0.90$; $n = 5$) and a weaker correlation with liptinite contents ($r^2 = 0.58$) suggest that vitrinite reflectance is suppressed due to bitumen generated from liptinites (Diessel, 1992).

Vitrinite percentages range from 56% to 82%. A high proportion of vitrinite displays a considerable fluorescence. Liptinite contents increase upwards from 6% to 13%. The average liptinite content is about 10%. Inertinite percentages are also relatively high. Sample 4 (0.9 m above the base of the seam; Fig. 12d) contains 32% inertinite. Degradofusinite, macrinite, and pyrofusinite are the most abundant

inertinite macerals. The VI is about 1.0 near the base and the top of the seam and is considerably below 1.0 in the middle part. The average VI (0.85) is lower than in any other studied Moscovian seam. GWI and GI are also low. The GI shows a general upward decrease but increases in the uppermost sample.

4.2. Organic geochemistry

4.2.1. Rock Eval pyrolysis

The maturity parameter T_{max} correlates well with vitrinite reflectance ($r^2 = 0.93$; $n = 71$; Fig. 13a). The trend line is similar to that published by Teichmüller and Durand (1983) and Veld et al. (1993). However, high-rank Donets coals (l_1 and m_3 seams in the 13bis and Bazhanova mines) tend to have slightly higher T_{max} values at a given vitrinite reflectance.

HI values of coal range from 120 to 310 mgHC/gTOC. HI values of mudstone (50–234 mgHC/gTOC) are often significantly lower than that of coal in the same profile. A plot of HI against vitrinite reflectance (Fig. 13b) shows that HI of coal is mainly controlled by maturity.

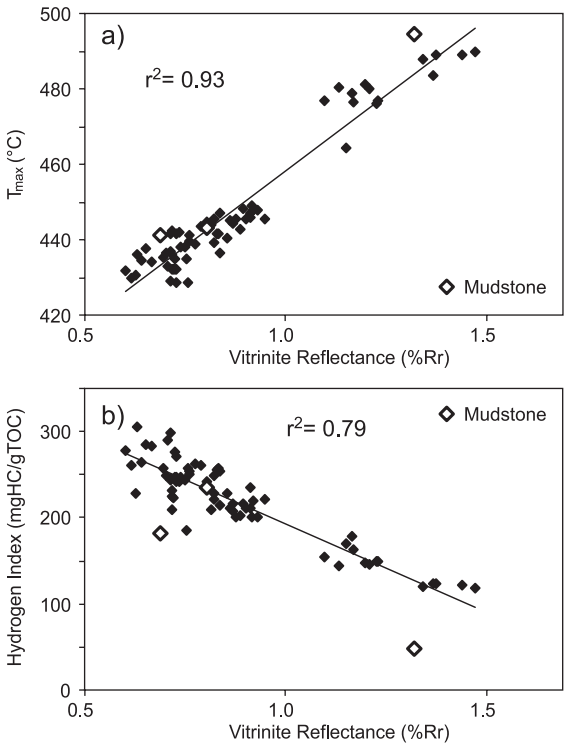

Fig. 13. Vitrinite reflectance versus (a) T_{max}, and (b) hydrogen index for Donets Basin samples.

Within-seam variations of HI are shown in Figs. 3, 7, 9, and 10. HI values increase upwards from 230 to 280 mgHC/gTOC in the c_{10}^2 seam. In the $m_5^{1\ upper}$ seam (185–246 mgHC/gTOC) the lowest HI value occurs in the ash-rich middle part of the seam. In most other seams there are only minor vertical variations. The highest average HI (282 mgHC/gTOC) occurs in seam m_2 in the Belitskaya mine. In a few seams HI displays correlations with macerals. However, in most seams there is no correlation. Littke and ten Haven (1989) made similar observations and assumed that this is because high liptinite contents are often associated with high inertinite percentages.

4.2.2. Extract characterisation

Typical *n*-alkanes, isoprenoids, hopanes, and steranes distributions in extracts from Donets Basin coals are presented in Fig. 14. Peak assignments are shown in Table 3 and important geochemical parameters are summarized in Table 4. Selected data for the l_1 and n_1 seams are plotted versus depth in Fig. 15.

4.2.2.1. Extract yields and distribution of polars, aromatics and aliphatics. The yields of extractable organic matter range from 1.5 to 22 mg/g of coal. The highest value occurs in the l_1 seam below the shaly seam split. This sample is also characterized by an exceptionally high S1 value. Nevertheless, extraction yields are low compared to coals from the Lorraine Basin in France (5–40 mg/g; Fleck et al., 2001).

The extracts contain high relative proportions of polar compounds (51–83%), medium proportions of aromatic components (14–38%) and low amounts of aliphatic hydrocarbons (3–12%). Asphaltenes predominate within the polar fraction (25–51%). The ratio between the aromatic and aliphatic fractions varies from 2.8 to 5.8. The uppermost sample in the n_1 seam contains more aromatic (37%) and aliphatic hydrocarbons (8%) than the deeper samples.

In the l_1 seam, samples with low extract yields (3, 4, 9) show higher concentrations of aromatic and aliphatic hydrocarbons than other samples. The Serpukhovian seams c_{10}^2 and c_{11} also contain high amounts of aromatic and aliphatic hydrocarbons

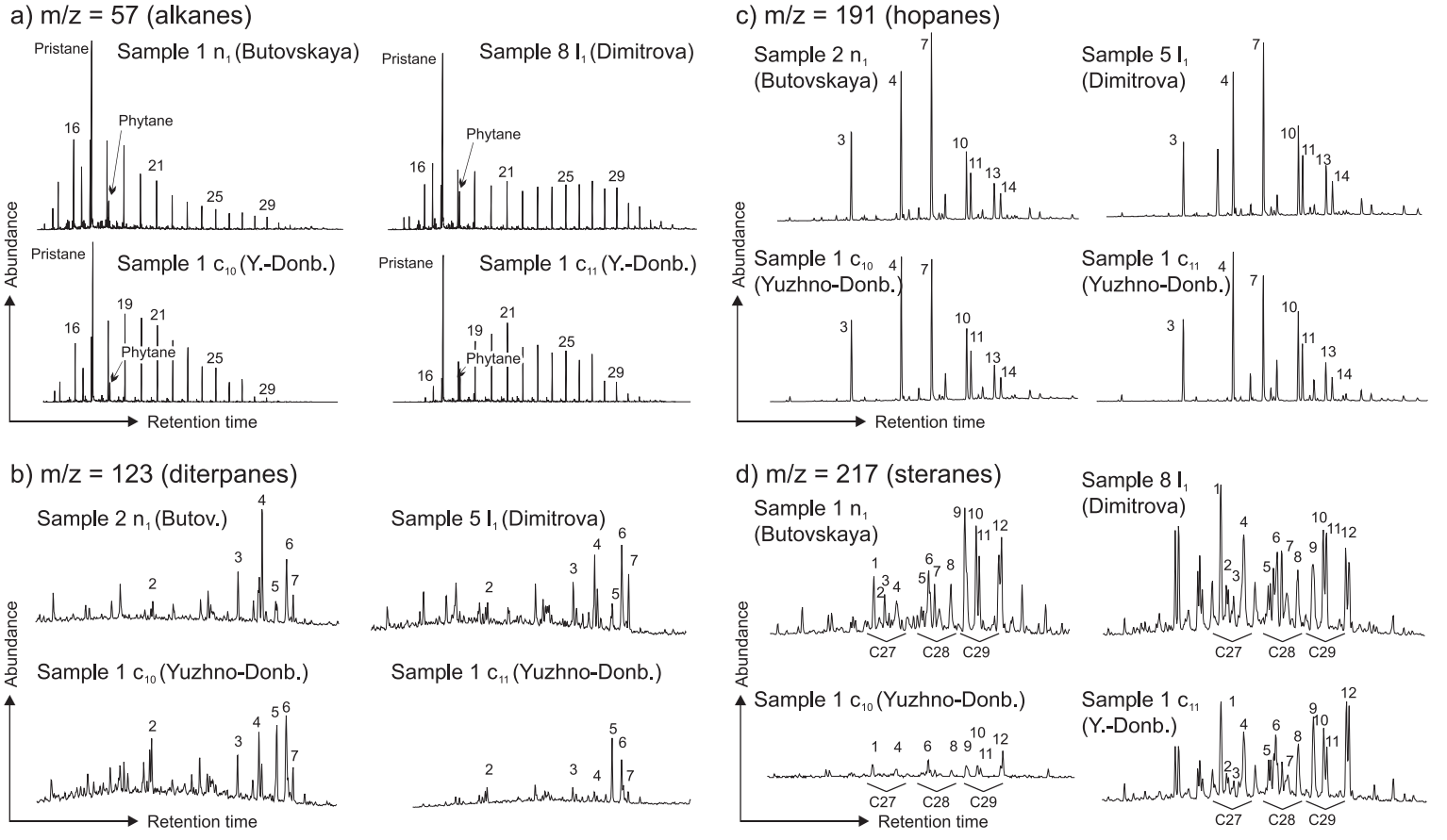

Fig. 14. Examples of (a) *n*-alkanes and isoprenoid distributions (*n*-alkanes are labeled according to their carbon numbers), (b) diterpane distributions, (c) hopane distributions, and (d) sterane distributions of typical Donets coals. Peaks are identified in Table 3.

Table 3
Peak assignments for diterpanes, hopanes and steranes

Peak number	Name
Diterpanes	
2	19-Norisopimarane
3	*ent*-Beyerane
4	*iso*-Pimarane
5	16β-Phyllocladane
6	16α-Kaurane
7	16α-Phyllocladane
Hopanes	
3	Trisnorhopane (C_{27})
4	Norhopane (C_{29})
7	Hopane (C_{30})
10	22*S*-homohopane (C_{31})
11	22*R*-homohopane (C_{31})
13	22*S*-bishomohopane (C_{32})
14	22*R*-bishomohopane (C_{32})
Steranes	
1	α-Cholestane(20*S*)C_{27}
2	β-Cholestane(20*R*)C_{27}
3	β-Cholestane(20*S*)C_{27}
4	α-Cholestane(20*R*)C_{27}
5	Methyl-α-Cholestane(20*S*)C_{28}
6	Methyl-β-Cholestane(20*R*)C_{28}
7	Methyl-β-Cholestane(20*S*)C_{28}
8	Methyl-α-Cholestane(20*R*)C_{28}
9	Ethyl-α-Cholestane(20*S*)C_{29}
10	Ethyl-β-Cholestane(20*S*)C_{29}
11	Ethyl-β-Cholestane(20*S*)C_{29}
12	Ethyl-α-β-Cholestane(20*R*)C_{29}

(46–49%). In general, aromatic and aliphatic hydrocarbons (17–49%) are higher in coals from the Donets Basin than from the Lorraine Basin (Fleck et al., 2001).

4.2.2.2. n-Alkanes distributions. The mass chromatograms ($m/z=57$) for the *n*-alkanes for selected samples are shown in Fig. 14a. The *n*-alkane distributions are generally unimodal with maximum peaks between *n*-C_{16} and *n*-C_{19}. The abundance of longer chain *n*-alkanes decreases exponentially with chain length. Only in coal from the c^2_{10} seam and in sample 8 from the l_1 seam (Dimitrova section) do longer chain *n*-alkanes occur in significant percentages. Similar patterns have been documented in Carboniferous coals and coaly rocks with a similar maturity from the Ruhr (Littke and ten Haven, 1989) and Lorraine basins (Fleck et al., 2001).

The Carbon Preference Index (CPI; Bray and Evans, 1961) ranges from 1.04 to 1.23 in the l_1 and n_1 seams and is slightly higher in seams c^2_{10} and c_{11}. Average CPI values for different seams correlate well with thermal maturity parameters (Rr: $r^2=0.89$; T_{max}: $r^2=0.95$; $n=4$) indicating that differences in CPI are mainly controlled by differences in maturity.

The relative abundances of short-chain (*n*-C_{17-19}) and long-chain (*n*-C_{25-34}) *n*-alkanes have been quantified (Table 4; Fig. 15). The abundance of *n*-C_{15-19} alkanes is an indicator of algal organic matter and the abundance of *n*-alkanes higher than C_{22} is an indicator of wax of higher plants (Tissot and Welte, 1984). However, a predominance of *n*-C_{15-20} alkanes can also reflect bacterial biomass input or biodegradation of *n*-alkanes during coal deposition (Peters and Moldowan, 1993).

Maturation also results in a shift towards short-chain *n*-alkanes. Thus, it is difficult to compare coals with different maturity. However, within-seam variations in the l_1 seam suggest that different organic matter input and/or different bacterial overprint contributed to the different *n*-alkane patterns. Because alginite is rare in the l_1 seam, the reduced amount of long-chain *n*-alkanes and the low HI value of sample 8 from this seam may indicate less severe bacterial activity.

4.2.2.3. Isoprenoids. Pristane/phytane (Pr/Ph) ratios range from 5 to 10. On average, slightly higher values are observed in the n_1 and c^2_{10}, than in the l_1 and c_{11} seams. In oxic conditions, the transformation of phytol to pristane is favoured, resulting in Pr/Ph ratios higher than 1. On the contrary, a ratio below 0.6 is related to anoxic conditions (Volkman and Maxwell, 1986). The results clearly indicate oxic conditions for all coals. Because Pr/Ph ratios are known to be affected by thermal maturity (e.g. Tissot and Welte, 1984), it is difficult to compare ratios from different seams. However, within-seam variations can be interpreted in terms of varying redox conditions. Accordingly, the observed upward increase in the n_1 seam (6.8–9.3; Fig. 15) indicates more oxic conditions in the uppermost part of the seam. Within the l_1 seam Pr/Ph ratios (5.2–7.6) indicate considerable vertical variations of redox conditions below the fluvial seam split. In this part of the seam, Pr/Ph

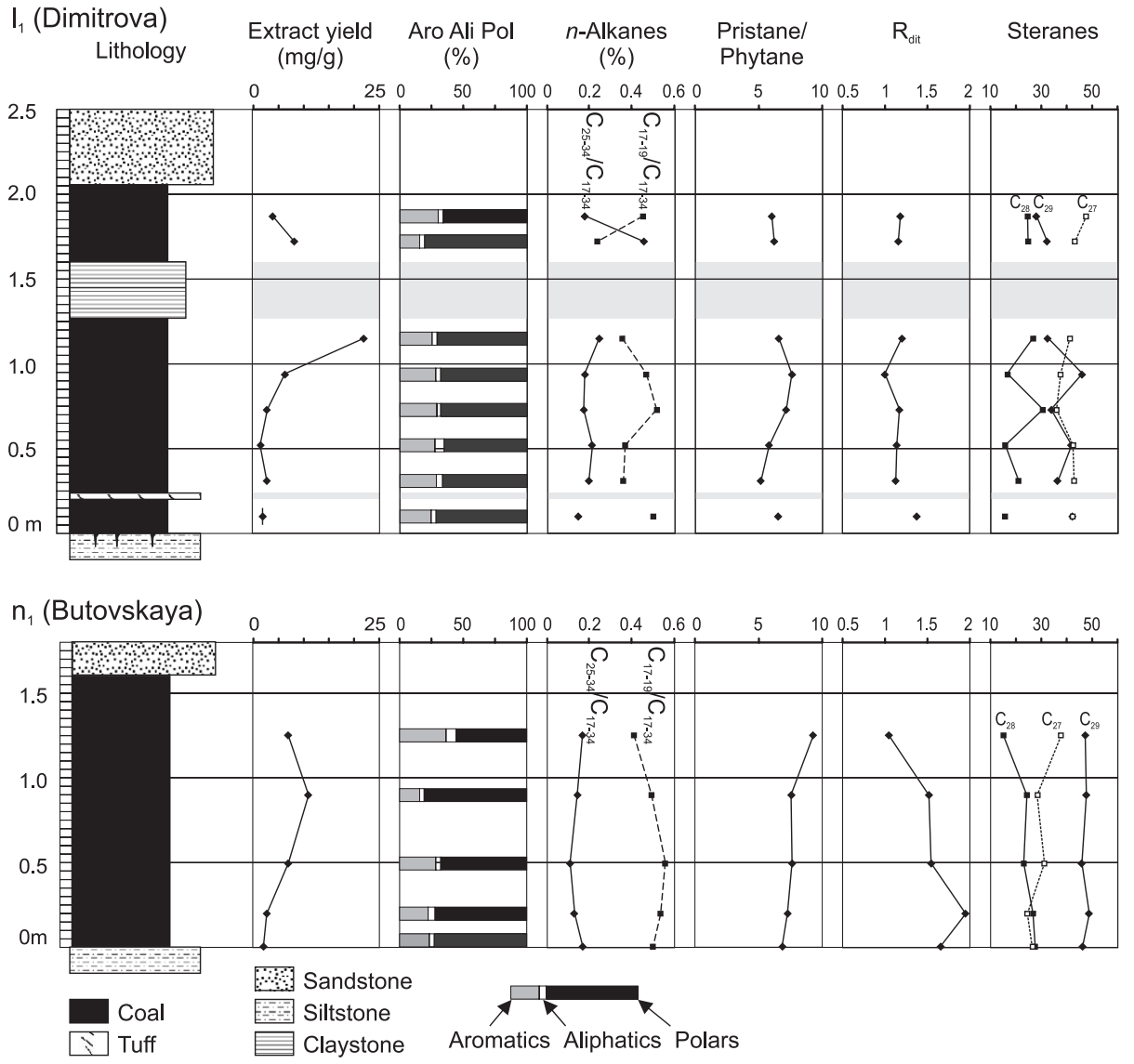

Fig. 15. Depth trends of extract yield, relative proportions of different hydrocarbon fractions, relative proportions of short chain and long chain *n*-alkanes to total *n*-alkanes contents, pristane/phytane ratio, the R_{dit} ratio (see text for details), and relative proportions of steranes with different carbon numbers in seams l_1 (Dimitrova) and n_1 (Butovskaya).

ratios correlate well with inertinite percentages ($r^2 = 0.81$; $n = 6$). The correlation is worse in the upper part of the seam.

The Pr/*n*-C_{17} ratio is generally between 3 and 6 but exceeds 10 in the c_{11} seam and in the uppermost n_1 seam. The Ph/*n*-C_{18} ratio ranges from 0.35 (c^2_{10}) to 1.13 (n_1). The ratios are in accordance with the postulated deposition in a mire (Lijmbach, 1975; Connan, 1981).

4.2.2.4. Diterpanes. Diterpanes were detected in the $m/z = 123$ chromatograms. The determination was made by comparing chromatograms and mass-spectra diagrams from Noble et al. (1985a,b). The following

Table 4
Extraction yield, relative proportions of asphaltenes, NSO (polars without asphalthenes) and polars (total), aromatic and aliphatic compounds in the extract

Sample	Bulk bitumen parameters							*n*-alkanes			Isoprenoids			Diterpanes	Steranes		
	Extract (mg/g)	Asphaltenes	NSO	Polars	Aromatics	Aliphatics	Aromatics/ aliphatics	n-$C_{17\text{-}19}$/ n-C_{17-34}	n-C_{25-34}/ n-C_{17-34}	CPI	Pr/Ph	Pr/n-C_{17}	Ph/n-C_{18}	R_{dit}	C_{27}	C_{28}	C_{29}
		wt.%													wt.%		
n_1 (Butovskaya)																	
5	7.0	37	18	55	37	8	4.6	0.41	0.17	1.23	9.31	10.77	1.13	1.05	37.7	15.1	47.2
4	11.0	42	41	83	14	3	4.7	0.49	0.14	1.11	7.56	5.48	0.70	1.52	28.3	24.1	47.6
3	7.0	46	20	66	29	5	5.8	0.56	0.11	1.14	7.66	3.42	0.47	1.54	31.2	23.0	45.9
2	2.7	44	28	72	22	6	3.7	0.53	0.13	1.15	7.26	4.32	0.61	1.95	24.4	26.7	48.9
1	2.1	41	29	70	25	5	5.0	0.50	0.17	1.15	6.88	3.13	0.48	1.66	26.3	27.6	46.1
l_1 (Dimitrova)																	
9	4.0	41	25	66	28	6	4.7	0.45	0.18	1.11	6.02	5.33	0.91	1.18	47.6	24.5	27.9
8	8.2	34	46	80	14	6	2.3	0.24	0.46	1.03	6.20	5.84	0.98	1.16	43.1	24.7	32.2
6	22.1	49	21	70	25	5	5.0	0.35	0.24	1.20	6.57	4.52	0.73	1.20	41.0	26.6	32.4
5	6.4	46	22	68	26	6	4.3	0.47	0.18	1.16	7.62	5.84	0.81	1.00	37.5	16.4	46.1
4	2.9	41	22	63	31	6	5.2	0.51	0.17	1.10	7.16	4.33	0.71	1.17	35.7	30.5	33.7
3	1.5	41	20	61	30	9	3.3	0.36	0.21	1.11	5.80	5.56	0.79	1.14	42.4	15.7	41.9
2	2.8	48	19	67	27	6	4.5	0.36	0.19	1.15	5.16	6.08	0.87	1.13	42.8	20.9	36.4
1	2.0	51	17	68	25	7	3.6	0.50	0.15	1.11	6.56	6.12	0.95	1.38	42.1	15.8	42.2
c_{11} (Yuzhno-Donbasskaya #3)																	
	8.6	29	25	54	34	12	2.8	0.18	0.33	1.25	5.94	10.54	0.96	0.78	37.2	29.0	33.9
c^2_{10} (Yuzhno-Donbasskaya #1)																	
1	7.7	25	26	51	38	11	3.5	0.41	0.14	1.57	9.51	3.81	0.35	1.17	30.4	30.6	39.0

Aromatic to aliphatic hydrocarbon ratios, relative intensities of short and long chain *n*-alkanes, carbon preference index (CPI; after Bray and Evans, 1961). Pristane/phytane (Pr/Ph) ratio, and ratios of pristane/n-C_{17}, and phytane/n-C_{18}, R_{dit} ratio after Fleck (2001), and relative proportions of C_{27}, C_{28}, C_{29} steranes.

diterpanes were detected (numbers refer to diagrams in Fig. 14b):

(2) 19-Norisopimarane, (3) *ent*-Beyerane, (4) *iso*-Pimarane, (5) 16β-Phyllocladane, (6) 16α-Kaurane and (7) 16α-Phyllocladane.

According to Philp (1994) diterpanes occur in the following groups of Carboniferous plants:

- Pimaranes (2 + 4): pre-gymnosperms (cordaites), pteridophytes, bryophytes;
- *ent*-Beyerane (3): pre-gymnosperms;
- Kaurane (6): pre-gymnosperms, pteridophytes, bryophytes;
- Phyllocladanes (5 + 7): pre-gymnosperms.

Fleck (2001) suggested a diterpane ratio (R_{dit}), which is a measure for the relative abundance of pteridophytes and for the height of the water table in the mire (low: $R_{dit} < 1$; medium to high: $R_{dit} > 1$).

$$R_{dit} = \frac{\text{19-Norisopimarane} + \textit{iso}\text{-Pimarane} + 16\alpha\text{-}\textit{Kaurane}}{\textit{ent}\text{-Beyerane} + 16\text{h-Phyllocladane} + 16\text{a-Phyllocladane}}$$

The lowest R_{dit} ratio occurs in the c_{11} seam (0.78). The c^2_{10} and l_1 seams are characterized by medium ratios (1.0–1.4), whereas relatively high values prevail in the n_1 seam (1.05–1.95). No vertical trend is visible within the l_1 seam, but sample 5 differs in a reduced R_{dit} ratio (1.0; Fig. 15). In the n_1 seam the R_{dit} ratio decreases upwards. In both seams, the samples with the highest relative abundance of pre-gymnosperm-derived biomarkers (low R_{dit} values) are the samples with the highest Pr/Ph ratio. This agrees with the interpretation that low R_{dit} ratios reflect low water tables favouring oxic conditions.

4.2.2.5. Hopanes. Hopanes are ubiquitous constituents of sedimentary organic matter. They are derived from the degradation of the bacteriohopane C_{35} (Ourisson et al., 1979). A unimodal distribution of hopanes with a maximum at C_{30} was found in all samples. The abundance of hopanes above C_{31} decreases progressively. Hopanes are characteristic for the presence of bacteria in the swamp (Ourisson et al., 1979) and the hopanes distribution indicates an oxic-type paleoenvironment (Philp and Mansuy, 1997).

4.2.2.6. Steranes. The distributions of C_{27}, C_{28} and C_{29} steranes are plotted versus depth (Fig. 15) and are

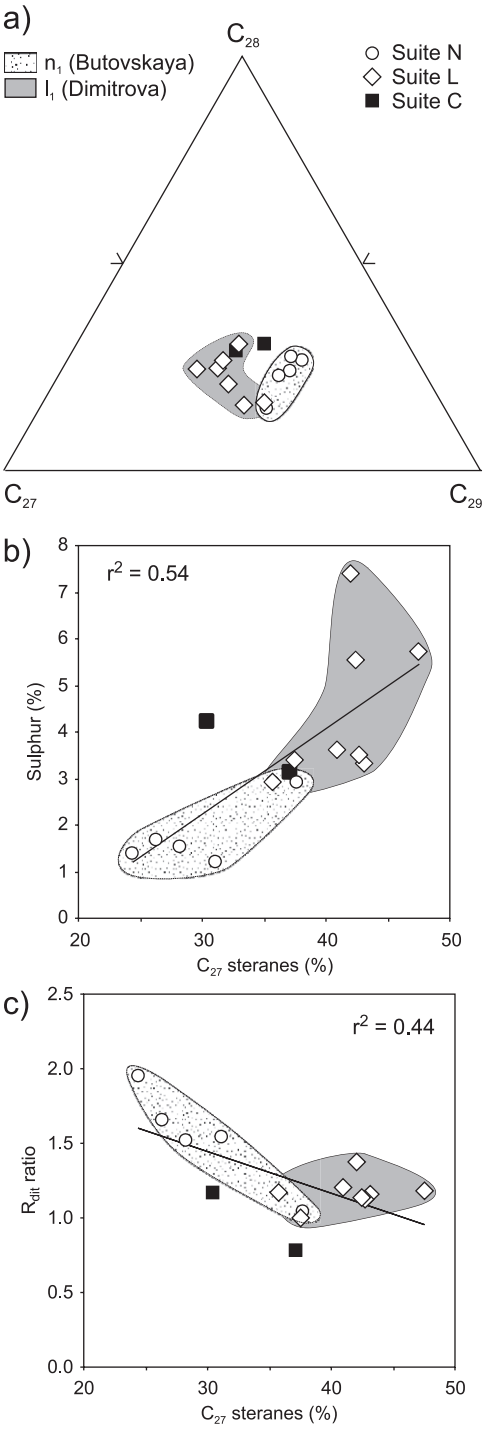

Fig. 16. Sterane data. Sterane carbon number distributions for coals from c^2_{10}, c_{11}, l_1 and n_1 seams (a). Plot of relative proportions of C_{27} steranes versus sulphur content (b) and R_{dit} ratio (c).

displayed in a ternary diagram (Fig. 16a). The n_1 seam is characterized by a dominance of C_{29} steranes (45–49%) without any vertical trend. C_{27} steranes increase upwards from 24% to 38%, whereas C_{28} steranes decrease in the same direction (28–15%). Sterane patterns in the l_1 seam are more variable and C_{27} steranes are more abundant. Only sample 5 is dominated by C_{29} steranes. C_{27} steranes increase and C_{29} steranes decrease in the upper part of the coal seam. Coal samples from suite C are characterized by equal amounts of C_{27}, C_{28} and C_{29} steranes. Percentages in C_{27} steranes correlate with sulphur contents ($r^2 = 0.54$; $n = 15$; Fig. 16b), and decrease with increasing R_{dit} ratios ($r^2 = 0.44$; $n = 15$; Fig. 16c).

C_{29} steranes in coals are mainly derived from C_{29}-sterols from the wood of higher plants. C_{27} and C_{28} steranes can be indicative of algal-derived kerogen (e.g. Huang and Meinschein, 1978, 1979). The C_{27} and C_{28} steranes may also be derived from heterotrophs (protozoa, fungi, various invertebrates) decomposing wood, or bacteria degrading C_{29} sterol chains. Maturity effects probably have little influence on the distribution of C_{27}, C_{28} and C_{29} steranes within the present maturity range (0.6–0.8% Rr; see Dzou et al., 1995).

The correlation of C_{27} percentages with sulphur contents suggests a relation between (sulphur-reducing) bacteria and the concentrations of C_{27} steranes. Therefore, and because alginite is rare, a bacteria-derived origin of C_{27} steranes in Donets Basin coals is likely.

5. Discussion

5.1. Paleoenvironmental interpretations

5.1.1. Serpukhovian seams

The fine-grained floor and roof rocks of early Serpukhovian (Stechevskian–Tarussian) seams c_{10}^2 and c_{11} were deposited in lagoons (Shulga, 1981). The coal is rich in inertinite (20–30%) and liptinite (15–25%) and very low in ash. GWI, VI, and GI are likewise low and lower than in any studied Moscovian seam. Average maceral group percentages of the studied seams fit well those of seams c_2 and c_6^1 (Volkova, 1975). In the latter two seams inertinite contents increase from the base (~10%) towards the top of the seam (40–50%; Volkova, 1975). A similar trend is visible in seam c_{10}^2 and suggests that each of these Serpukhovian seams represents an evolutionary trend to drier and less groundwater influenced conditions. Relatively dry conditions and highly oxidized peat are also indicated by the frequent occurrence of herbaceous lycopods (*Densosporites*) which, together with arborescent lycopods (*Lepidodendron*, *Lagenicula*), dominate Serpukhovian plant and palynomorph spectra from the Donets Basin (Einor, 1996).

According to Shulga (1981), the southwestern margin of the Donets Basin (tectonic sector D1 after Privalov et al., 1998) subsided rapidly during coal deposition. This caused marine ingressions from the central basin and the transport of high amounts of clastic sediments by northeastward trending rivers, which dissected the approximately 10-km-wide, NW–SE trending zone with peat accumulation. Although the coal was formed in a relatively narrow shore-zone surrounded and dissected by high energy environments, the coal seams are depleted in mineral matter. This, together with a trend towards less groundwater influence, suggests peat accumulation in raised mires.

The studied samples contain significantly more sulphur (1.8–4.2%) than typical raised mires. However, lower average sulphur contents are reported from the Yuzhno Donbasskaya mines (e.g. 1% in the c_{11} seam; Triplett et al., 2001) indicating major regional differences in sulphur. Probably, the observed high sulphur contents are a result of marine flooding events, which ended peat accumulation. In addition, sulphur (and trace element) maxima at the base of the c_{10}^2 seam may be a result of diffusion processes or plant-root bioturbation.

5.1.2. Moskovian seams

Izart et al. (1996) subdivided the Moscovian succession into 4 third-order sequences (Vereian, Kashirian, Podolskian, Myachkovian) and 18 fourth-order sequences (SM1-SM18). In the present chapter, typical features of Kashirian, Podolskian, and Myachkovian seams are described. Information on the depositional environment of the floor and roof rocks is taken from Ritenberg (1972).

5.1.2.1. Kashirian seams. Seams k_7, l_1, and l_3 occur in the Kashirian succession, which includes some of the thickest seams with the greatest lateral extension

in the Donets Basin. For example, according to reconstructions by Kizilshtein (1975), the original aerial extent of the l_3 seam exceeded 35,000 km^2. In spite of the vast area, the remarkable persistent position of tuff markers in the l_1 and l_3 seams (Fig. 6; Zaritsky, 1972) confirms roughly contemporaneous peat accumulation in different parts of the basin. The maximum thickness of the seams exceeds 2 m. However, in some areas the seams have been eroded by fluvial activity.

Seam k_7. In comparison with other Kashirian seams, the low-ash k_7 seam is relatively thin. GI is high suggesting a low degree of oxidation. High VI values near the base of the seam indicate that conditions for tissue preservation were best during early stages of peat formation. The virtual absence of detrital minerals and a generally low sulphur content suggest either deposition in a raised mire or in a low-lying mire without detrital influx. The low sulphur content excludes a marine influence during early stages of peat accumulation. This interpretation is in agreement with paleogeographic reconstructions. Zhemtchuzhnikov et al. (1960) show that the western margin of the marine realm was distant from the study area and followed roughly the line Kamensk-Krasny Luch-Novoshakhtinsk during deposition of the k_7 seam. Siltstone, probably of lacustrine origin (Ritenberg, 1972), forms the roof of the seam. This suggests that peat formation ended due to a transgression. The latter is supported by higher sulphur (2.3%) and liptinite contents in the uppermost part of the seam (e.g. Diessel, 1992). However, the high sulphur value supports a brackish rather than a non-marine transgression.

Seam l_1. In the study area, the l_1 seam overlies a roughly 30-m-thick fining-upward sequence with fluvial conglomerate and sandstone and limnic claystone. The roof of the seam is formed by lagoonal claystone a few meters thick (Ritenberg, 1972). Because of the influence of sulphate-rich water during or after peat accumulation, the sulphur contents of the coal are generally high. The seam is located within the regressive part of SM4 but close to the maximum flooding surface of the third-order sequence Kashirian (Izart et al., 1996). This may explain the sulphur enrichment for seam l_1. After deposition of the lagoonal shale, fluvial systems cut into the shale and eroded parts of the l_1 seam (see Fig. 6).

Relatively high ash yields and occasional seam splits show that the l_1 seam formed in a low-lying mire. GWI, GI, and Pr/Ph ratios suggest relatively dry and oxic conditions during early stages of peat formation, which were modified only during a rise in water table after deposition of the tuff layer. The major seam split is related to east-trending rivers dissecting the vast peatland (Zhemtchuzhnikov et al., 1960). High inertinite contents and low GI values suggest that relatively dry conditions continued after deposition of the fluvial sediments in the Dimitrova region. However, high ash yields provide evidence for frequent flooding events. VI values show that there was little change in the relative proportion of plants with different preservation potential. Nevertheless, a weak positive correlative exists between VI and R_{dit} ($r^2 = 0.53$; $n = 8$) suggesting that pteridophytes are more decay resistant than other plants.

Seam l_3. The l_3 seam overlies seam l_2 and lacustrine claystone (Ritenberg, 1972). The roof is formed by lagoonal claystone followed by another coal seam (l_4). In some areas the lagoonal claystone interfingers with fluvial sandstone deposited in easterly flowing drainage systems (Zhemtchuzhnikov et al., 1960). In the central and eastern Donets Basin the roof of the l_3 seam is formed by marine limestone L_4 (Uziyuk et al., 1972).

In the studied section the l_3 seam contains two tuff layers and several partings, which suggest peat deposition in a low lying mire. The GI shows parallel trends in both sections, indicating that the ratio between vitrinite and inertinite reflects large-scale variations within the seam. Generally, high GI values in the lower portions of the seam indicate a high position of the water table. Probably, the mire became drier between the deposition of the lower and upper tuffs. VI values range from 1 to 2 and suggest a vegetation rich in decay resistant trees.

Whereas facies indicators are similar in both sections, there is a difference in sulphur contents. Sulphur contents are higher in the Belozerskaya (2.8%) than in the Almaznaya section (1.3%). An even wider range of sulphur contents was observed by Kizilshtein (1975), who suggested a raised mire environment for low-sulphur coals (<1.5%). High-sulphur coals (>3.5%) with high ash yields were interpreted to have formed near shallow, mainly E–W trending depressions formed by intra-swamp rivers, which

were regularly flooded by marine water. Because original data were not shown by Kizilshtein (1975), it is difficult to test this interesting model. However, the studied sections exhibit similar seam thicknesses and similar coal facies. This argues against a control of sulphur by peat facies in the present case. Moreover, frequent seam splitting excludes a raised mire environment for the bulk of the Almaznaya coal. According to Izart et al. (1996), the seam is located within the regressive part of SM5. This may explain the lack of a sulphur enrichment at the top of the seams.

Moderately high ash yields in the uppermost part of the seam result from epigenetic carbonate and minor amounts of authigenic quartz. Zones with high amounts of authigenic quartz in the Belitskaya and Belozerskaya mines are shown in Fig. 6 (“quartzitic coal”; Uziyuk et al., 1972). The spatial relation of quartz and tuff argues for a genetic link. Perhaps, the silica became available during the transformation of tuff material into kaolinite. Siderite was described by Uziyuk et al. (1972) from the uppermost portion of the l_3 seam but was not detected in the studied sections.

5.1.2.2. Podolskian seams. Seams m_2, m_3, and $m_5^{1\ upper}$ were deposited during Podolskian times. The first two seams overlie lagoonal deposits and are overlain by lagoonal and marine rocks (Ritenberg, 1972) suggesting that peat accumulation ended due to a marine transgression. This fits well with the position of both seams within the transgressive part of the third-order sequence Podolskian close to the Moscovian maximum flooding period (Izart et al., 1996). Very high average sulphur contents (>4%) and high HI values (m_2) indicating high hydrogen contents are consistent with a marginal marine environment (e.g. Diessel, 1992). The marine influence reduced the acidity of the peat. High CaO contents in some samples are consequences of these conditions. Ash from the m_2 seam has higher SiO_2/Al_2O_3 ratios than that of most other seams (except those with authigenic quartz). Perhaps this indicates a better preservation of detrital silicate minerals, another result of nearly neutral or slightly alkaline pH conditions. Although the acidity of the mire was probably reduced, the mire was still acidic enough to convert the tuff layer a few centimetres below the top of the m_3 seam into kaolinite.

The seam m_2 contains high-ash coal, which was deposited in a low-lying mire. A shaly seam split represents a major flooding event. VI values are low compared to other Moscovian seams suggesting a relatively low contribution of decay-resistant plants to the peat-forming vegetation. GI values indicate a gradual drop in water table during both deposition of the lower and of the upper part of the seam. However, several other properties of the uppermost portion of the seam (upward increase in GWI, sulphur and liptinite contents, decrease in vitrinite reflectance and VI) are characteristic for transgressive coals (e.g. Diessel, 1992).

Peat facies reconstruction for the m_3 seam are complicated by the advanced maturity of the studied section. However, cannel and cannel-boghead coal, characteristic of subaquatic deposition, occur in the upper part of the seam in the southern Krasnoarmeisk region (Yablokov et al., 1955). Authigenic quartz is abundant in the middle part of the m_3 seam in the studied section. The authigenic quartz is related to bitumen, which is strongly fluorescing despite the high coal rank. This suggests that bitumen migration and quartz growth postdate the thermal maximum. This interpretation agrees with a late diagenetic origin of authigenic quartz postulated by Zaritsky (1985).

In contrast to the above seams, the $m_5^{1\ upper}$ seam in the Almaznaya section is under- and overlain by lacustrine claystone. Detrital minerals in the coal are generally rare. High ash yields in the middle part of the seam partly result from epigenetic pyrite. Apart from this sample, sulphur contents are moderate (<2%), a consequence of the nonmarine environment.

5.1.2.3. Myachkovian seam n_1. The seam n_1 was deposited during the regressive phase of SM17 (Izart et al., 1996) and is the youngest economic seam in the Donets Basin. Mainly because of erosion during the lowstand of SM18 and during major Permian uplift, its present-day areal extent is low. In the studied section the n_1 seam is overlain by fluvial sandstone (Ritenberg, 1972).

Moderate sulphur contents in the bulk of the seam (1.2% to 1.7%) indicate that the peat was not influenced by marine water. However, the sulphur content increases significantly in the uppermost part of the

seam. This, an upward increase in HI, and GI, and an upward decrease in vitrinite reflectance suggest peat accumulation during a transgression. Inertinite contents are higher than in any other Moscovian seam. This causes relatively low GI values and indicates, together with very high Pr/Ph ratios, rather dry and oxic conditions. The regular upward increase in Pr/Ph ratios suggests a trend to even more oxic conditions during peat deposition. The R_{dit} ratio suggests that the relative abundance of bryophytes and pteridophytes decreased during peat accumulation. Perhaps this is because of a gradual drop in water table, indicated by the increasing Pr/Ph ratio. The postulated floral change is not reflected in the VI data. The latter are lower in the n_1 seam than in most other Moscovian seams, indicating poor tissue preservation. Relatively low concentrations in C_{27} and C_{28} steranes suggest a minor contribution of bacteria and heterotrophs to the biomass.

R_{dit} ratios are generally higher in the Myachkovian n_1 seam than in Kashirian (l_1) and Serpukhovian (c^2_{10}, c_{11}) seams. Similar observations were made by Fleck (2001), who detected maximum R_{dit} ratios in Westphalian D (Podolskian and Myachkovian) coals from the Lorraine Basin. Apart from a higher proportion of bryophytes and pteridophytes, the raised R_{dit} ratio may indicate a wet climate (Fleck, 2001).

5.2. Possible reasons for different maceral compositions of Serpukhovian and Moscovian coals

Serpukhovian and Moscovian seams differ not only in terms of lateral extension but also in terms of maceral composition. The results from this study and previously published works show that Serpukhovian coals contain considerably higher amounts of liptinites and inertinites than Moscovian coals (Fig. 17a). The difference is also evident on crossplots of GI versus VI (Fig. 17b) and may be due to different peat facies, different climatic conditions, or different vegetation type.

High inertinite contents have been attributed to relatively dry conditions. Therefore, the generally higher inertinite contents in Serpukhovian coals could be attributed to local peat facies (e.g. relatively dry raised mires). However, Mississippian (Visean) coal from the Moscow Basin contains similar percentages of inertinite (30–35%; Volkova, 1975). Abundant

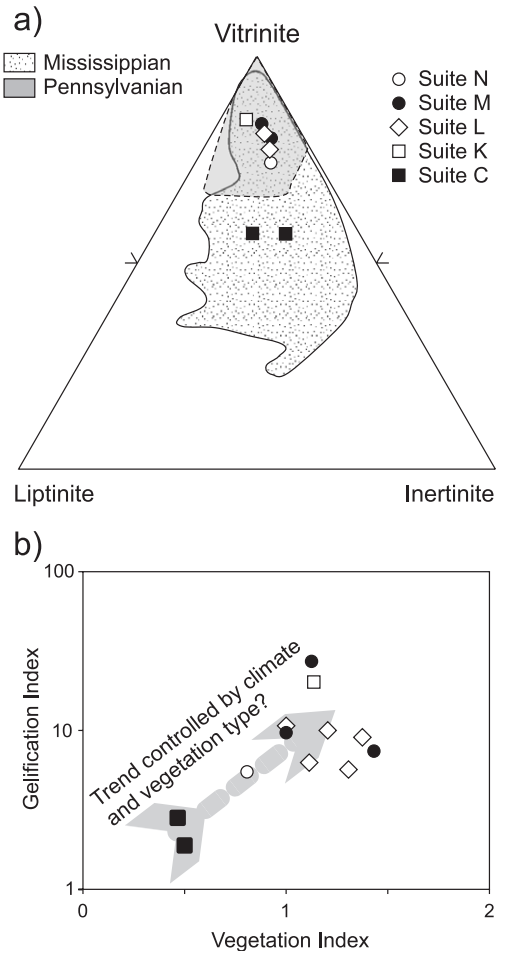

Fig. 17. (a) Comparison of average maceral group percentages in seams from different suites. Shaded areas indicate typical maceral compositions from lower and middle Carboniferous seams according to Inosova (1963). (b) Plot of the geometric mean of vegetation and gelification indices of different seams. Grey arrow indicates a stratigraphic trend, which is probably at least partly controlled by climate.

alginite and high ash yields prove the origin of this coal in a low lying mire suggesting that Mississippian coal from the eastern European platform contains abundant inertinite irrespective of local peat facies.

A relatively dry (moderately humid) Visean to early Serpukhovian climate is suggested by paleoclimatological models based on paleobotanical data. Van der Zwan (1981) and Van der Zwan et al. (1985) reconstructed a dry late Devonian to Tournaisian climate and a moderately humid Visean to early

Namurian climate. Phillips and Peppers (1984) showed that moist tropical conditions prevailed during Bashkirian and Moscovian times with maximum humidity during the late middle Pennsylvanian (Podolskian and Myachkovian). The late Pennsylvanian (Kasimovian) climate was transitional and was replaced by a dry late Stephanian and Permian climate. According to Van der Zwan et al. (1985), the changes in climate reflect a general northward shift of Euramerica.

The postulated climatic changes are also consistent with palynomorph spectra from the Donets Basin. Whereas Serpukhovian palynomorph spectra are dominated by arborescent and herbaceous lycopods, Moscovian spectra contain significant amounts of arborescent ferns, pteridosperms and lycopods. For example, Kashirian seams contain on average 50% spores from ferns and pteridosperms, 44% lycopods (*Lepidodendron*), 3% sphenopsids, and 3% cordaites (Lyuber, 1972).

The comparison suggests that the distinct differences in maceral compositions of Serpukhovian and Moscovian coals in the Donets Basin are probably attributable to climatic and floral changes rather than to local peat facies variations.

5.3. Distribution of trace elements

Correlation coefficients of trace elements are generally low, but Cu, Ni and Co are positively correlated. The highest correlation coefficient occurs between Ni and Co ($r^2 = 0.65$; $n = 51$). The correlation between Pb and Zn has a low coefficient ($r^2 = 0.44$; $n = 52$), which is higher, when only seams l_3 to n_1 are considered ($r^2 = 0.60$; $n = 36$).

Mo, Pb, Zn, and Cu are within the normal range of concentrations of these elements in ash from bituminous coals (e.g. Krejci-Graf, 1984; Table 2), although very high values are determined in some low-ash samples. Ni and Co are enriched only in the k_7 seam and at the base of the l_3 and n_1 seams. As mentioned earlier, the high values near the floor rocks may be due to plant-root bioturbation or diffusion processes.

In contrast, As and Cd contents are often significantly higher than in typical bituminous coals. A similar observation was made by Kizilshtein and Kholodkov (1999) in anthracites from the eastern Donets Basin (Russia). As contents between 2000 and 8000 ppm are observed in ash from samples from c^2_{10}, k_7, l_3 (Almaznaya), and m_3 seams. Most of the As is probably associated with pyrite (Hower et al., 1997). This is evident in seams c^2_{10} (only three samples) and n_1 ($r^2 = 0.99$; $n = 5$), where As is positively correlated with Fe. However, because not all pyrite morphologies have equal concentrations of As (e.g. Ruppert et al., 2001), there is not a good correlation between As and Fe for all other seams. Cd contents are very high (10–40 ppm) in ash from many samples. As contents increase upwards in the l_3 seam, but there is no distinct vertical trend in other seams. Cd contents also show neither vertical nor stratigraphical trends. Probably, this is because the observed very high As and Cd contents are related to post-Carboniferous magmatic activity and epigenetic Au, Hg, and Sb mineralizations (Lazarenko et al., 1975).

6. Conclusions

Formation of coal seams in the Donets Basin commenced during Serpukhovian time. Lower Serpukhovian coal accumulated in relatively small raised mires along the paleo-shore line and contains remarkably high inertinite and liptinite contents.

Moscovian seams have a considerably wider lateral extension (tens of thousands of square kilometres) and contain a significantly higher amount of vitrinite. Their properties vary widely in response to different peat facies. The Kashirian succession contains some of the thickest seams with the greatest lateral extension in the Donets Basin. For example, seams l_1 and l_3 are more than 2 m thick and were formed in low-lying mires with considerable fluvial influence. Podolskian seams were deposited close to the Moscovian maximum flooding period. A marine influence is apparent in several seams (e.g. m_2, m_3). The only economic Myachkovian seam (n_1) accumulated in a relatively dry swamp with a high proportion of bryophytes and pteridophytes.

Apart from local peat facies variations, differences between Serpukhovian and Moscovian coals reflect climatic and floral changes. In comparison to Serpukhovian times, the Moscovian was characterized by a wetter climate, and a vegetation rich in arborescent ferns, pteridosperms and lycopods.

Trace element contents are high in many seams. The distribution of Ni and Co suggests syn-depositional control (e.g. plant-root bioturbation), whereas very high As contents up to 8000 ppm are probably related to post-Carboniferous Au, Sb, and Hg mineralizations.

Acknowledgements

The authors express their gratitude to staff member from the coal mines for providing samples and additional geological information. Financial support by the Austrian Science Foundation (FWF project 14895) is gratefully acknowledged. A.S. was supported by the Austrian Exchange Service (ÖAD). The paper was improved considerably by the reviews of M. Mastalerz, an anonymous reviewer, and J. Hower.

References

Bechtel, A., Butuzova, L., Turchanina, O., Gratzer, R., 2002. Thermochemical and geochemical characteristics of sulphur coals. Fuel Processing Technology 77–78, 45–52.

Belokon, V.G., 1971. Geological history of evolution of the Donbas (in Russian). Geology and Prospecting of Coal Deposits. Nedra, Moscow, pp. 3–15.

Bray, E.E., Evans, E.D., 1961. Distribution of *n*-paraffins as a clue to recognition of source beds. Geochim. Cosmochim. Acta 22, 2–15.

Calder, J.H., Gibling, M.R., Mukhopadhyay, P.K., 1991. Peat formation in a Westphalian B piedmont setting, Cumberland basin, Nova Scotia: implications for the maceral-based interpretation of rheotrophic and raised paleomires. Bull. Soc. Geol. Fr. 162, 283–298.

Connan, J., 1981. Biological markers in crude oils. In: Mason, J.F. (Ed.), Petroleum Geology in China. Penwell, Tulsa, pp. 48–70.

Dehmer, J., 1995. Petrological and organic geochemical investigation of recent peats with known environments of deposition. Int. J. Coal Geol. 28, 111–138.

Deutsches Institut für Normung, 1978. Feste Brennstoffe; Bestimmung des Wassergehaltes, DIN 51718.

Deutsches Institut für Normung, 1980. Feste Brennstoffe; Bestimmung des Aschegehaltes, DIN 51719.

Diessel, C.F.K., 1986. On the correlation between coal facies and depositional environments. Proc. 20th Symp. Dep. Geol., Univ. Newcastle, N.S.W., pp. 19–22.

Diessel, C.F.K., 1992. Coal-Bearing Depositional Systems. Springer, Berlin. 721 pp.

Dzou, L.I.P., Noble, R.A., Senftle, J.T., 1995. Maturation effects on absolute biomarker concentration in a suite of coals and associated vitrinite concentrates. Org. Geochem. 23, 681–697.

Einor, O.L., 1996. The former USSR. In: Wagner, R.H. (Ed.), The Carboniferous of the World III, The Former USSR, Mongolia, Middle Eastern Platform, Afghanistan, and Iran. IUGS Publ., vol. 33. Instituto Geologico y Minero de España, Madrid, pp. 13–407.

Espitalié, J., Laporte, J.L., Madec, M., Marquis, F., Leplat, P.M., Paulet, J., Boutefeu, A.P., 1977. Méthode rapide de charactérisation des roches mères de leur potentiel pétrolier et de leur degré d'evolution. Rev. Inst. Fr. Pet. 32, 23–43.

Fleck, S., 2001. Corrélation entre géochimie organique, sédimentologie et stratigraphie séquentielle pour la caractérisation des paléoenvironnements de dépôt. PhD thesis, Université Henri Poincaré, Nancy 1. 387 pp.

Fleck, S., Michels, R., Izart, A., Elie, M., Landais, P., 2001. Paleoenvironmental assessment of Westphalian fluvio-lacustrine deposits of Lorraine (France) using a combination of organic geochemistry and sedimentology. Int. J. Coal Geol. 48, 65–88.

Hower, J.C., Robertson, J.D., Wong, A.S., Eble, C.F., Ruppert, L.F., 1997. Arsenic and lead concentrations in the Pond Creek and Fire Clay coal beds, eastern Kentucky coal field. Appl. Geochem. 12, 281–289.

Huang, W.-Y., Meinschein, W.G., 1978. Sterols in sediments from Buffin Bay, Texas. Geochim. Cosmochim. Acta 42, 1391–1396.

Huang, W.-Y., Meinschein, W.G., 1979. Sterols in sediments from Baffin Bay, Texas. Geochim. Cosmochim. Acta 42, 1391–1396.

Inosova, K.I., 1963. Petrographical characteristic of coal (in Russian). In: Kuznetzov, I.A. (Ed.), Geology of Coal Deposits and Coaly Shales of the USSR, vol. 1. Nedra, Moscow, pp. 297–322.

Izart, A., Briand, C., Vaslet, D., Vachard, D., Coquel, R., Maslo, A., 1996. Stratigraphy and sequence stratigraphy of the Moscovian in the Donets basin. Tectonophysics 268, 189–209.

Izart, A., Briand, C., Vaslet, D., Vachard, D., Broutin, J., Coquel, R., Maslo, A., Maslo, N., Kotzinskaya, R., 1998. Stratigraphy and sequence stratigraphy of the Upper Carboniferous and Lower Permian in the Donets Basin. In: Crasquin-Soleau, S., Barrier, É. (Eds.), Stratigraphy and Evolution of Peri-Tethyian Platforms. Peri-Tethys Memoir 3, vol. 177. Mémoires du Muséum National d'Histoire Naturelle, Paris, pp. 9–33.

Izart, A., Vachard, D., Vaslet, D., Maslo, A., 2002a. Sedimentology of the Upper Carboniferous and Lower Permian in the Dniepr and Donets Basins. In: Hills, L.V., Henderson, C.M., Bamber, E.W. (Eds.), Carboniferous and Permian of the World, XIV Int. Congress on the Carboniferous and Permian Proceedings. Can. Soc. Petrol. Geol. Memoir, vol. 19, pp. 120–143.

Izart, A., Vachard, D., Fauvel, P.-J., Vaslet, D., Kossovaya, O., Maslo, A., 2002b. Sequence stratigraphy of the Serpukhovian, Bashkirian and Moscovian in Gondwanaland, Western Europe, Eastern Europe, and USA. In: Hills, L.V., Henderson, C.M., Bamber, E.W. (Eds.), Carboniferous and Permian of the World, XIV Int. Congress on the Carboniferous and Permian Proceedings. Can. Soc. Petrol. Geol. Memoir, vol. 19, pp. 144–157.

Kizilshtein, L.Ya., 1975. Genesis of Sulphur in Coals (in Russian). Rostov Univ. Publ., Rostov. 200 pp.

Kizilshtein, L.Ya., Kholodkov, Yu.I., 1999. Ecologically hazardous elements in coals of the Donets Basin. Int. J. Coal Geol. 40, 189–197.

Krejci-Graf, K., 1984. Über die Elemente in Kohlen. Erdöl Kohle, Erdgas, Petrochem. Brennstoff-Chemie 37, 451–457.

Lazarenko, E.K., Panov, B.S., Gruba, V.I., 1975. The Mineralogy of the Donets Basin, 1 (in Russian). Naukova Dumka, Kiev. 225 pp.

Levenshtein, M.L., Spirina, O.I., Nosova, K.B., Dedov, V.S., 1991a. Map of Coal Metamorphism in the Donetsk Basin (Paleozoic surface). 1:500 000. Ministry of Geology of the USSR, Kiev.

Levenshtein, M.L., Lagutina, V.V., Kaminsky, V.V., 1991b. Explanations to the Maps of Thicknesses and Structure of Middle Carboniferous Coal Seams in the Donetsk Coal Basin (in Russian). Ministry of Geology of the USSR, Kiev. 100 pp.

Lijmbach, G.W.M., 1975. On the origin of petroleum. Proc. 9th World Pet. Congr. Applied Science Publ., London, pp. 357–369.

Littke, R., ten Haven, H.J., 1989. Paleoecologic trends and petroleum potential of Upper Carboniferous coal seams of western Germany as revealed by their petrographic and organic geochemical characteristics. Int. J. Coal Geol. 13, 529–574.

Lutugin, L.I., Stepanov, P.I., 1913. Donets Coal Basin. Review of Coal Deposits of Russia.

Lyuber, A.A., 1972. Palynological method (in Russian). In: Makedonov, A.V. (Ed.), Correlation of Coalbearing Sediments and Coal Seams in the Donets Basin. Nauka, Leningrad, pp. 48–57.

Marshall, J.S., Pilcher, R.C., Bibler, C.J., 1996. Opportunities for the development and utilization of coal bed methane in three coal basins in Russia and Ukraine. In: Gayer, R., Harris, I. (Eds.), Coalbed Methane and Coal Geology. Geol. Soc., Spec. Publ., vol. 109. The Geological Society, Bath, pp. 89–101.

Moore, T.A., Shearer, J.C., 2003. Peat/coal type and depositional environment—are they related? Int. J. Coal. Geol. (in press).

Nesterenko, L.P., 1978. Early Permian deposits of the Kalmius-Torets depression in the Donets Basin (in Russian). Vischa shkola, Kiev. 148 pp.

Noble, R.A., Alexander, R., Kagi, R.I., Knox, J., 1985a. Identification of some diterpenoid hydrocarbons in petroleum. Adv. Org. Geochem. 10, 825–829.

Noble, R.A., Alexander, R., Kagi, R.I., Knox, J., 1985b. Tetracyclic diterpenoid hydrocarbons in some Australian coals, sediments and crude oils. Geochim. Cosmochim. Acta 49, 2141–2147.

Ourisson, G., Albrecht, P., Maxwell, J.R., Wheatley, R.E., 1979. The hopanoids. Paleochemistry and biochemistry of a group of natural products. Pure Appl. Chem. 51, 709–729.

Panov, B.S., Dudik, A.M., Shevchenko, O.A., Matlak, E.S., 1999. On pollution of the biosphere in industrial areas: the example of the Donets coal Basin. Int. J. Coal Geol. 40, 199–210.

Peters, K.E., 1986. Guidelines for evaluating petroleum source rock using programmed pyrolysis. Am. Assoc. Pet. Geol. Bull. 70, 318–329.

Peters, K.E., Moldowan, J.M., 1993. The Biomarker Guide. Interpreting Molecular Fossils in Petroleum and Ancient Sediments Prentice-Hall, New Jersey. 363 pp.

Phillips, T.L., Peppers, R.A., 1984. Changing patterns of Pennsylvanian coal-swamp vegetation and implication of climatic control on coal occurrence. Int J. Coal Geol. 3, 205–251.

Philp, R.P., 1994. Geochemical characteristics of oils derived predominantly from terrigenous source materials. In: Scott, A.C., Fleet, A.J. (Eds.), Coal and Coal-Bearing Strata as Oil-Prone Source Rocks? The Geological Society, London, pp. 71–91.

Philp, R.P., Mansuy, L., 1997. Petroleum geochemistry: concepts, applications, and results. Energy Fuels 11, 749–760.

Popov, V.S., 1963. Tectonics of the Donets Basin (in Russian). In: Kuznetzov, I.A. (Ed.), Geology of Coal and Oil Shale Deposits of the USSR, vol. 1. Nedra, Moscow, pp. 103–151.

Privalov, V.A., Panova, E.A., Azarov, N.Ya., 1998. Tectonic events in the Donets Basin: spatial, temporal and dynamic aspects (in Russian). Geol. Geohim. Goruc. Kopalin (Geol. Geochem. Fossil Fuels) 4, 11–18.

Ritenberg, M.I., 1972. Method of the investigation of facies and cycles (in Russian). In: Makedonov, A.V. (Ed.), Correlation of Coalbearing Sediments and Coal Seams in the Donets Basin. Nauka, Leningrad, pp. 71–95.

Ruppert, L.F., Hower, J., Eble, C., Goldhaber, M., 2001. Local-scale Variability of Arsenic in the Fire Clay coal zone, Middle Pennsylvanian Breathitt Formation, eastern Kentucky: U.S. Geological Survey Workshop, Arsenic in the Environment, Feb. 21–22, 2001, Denver, CO. http://www.brr.cr.usgs.gov/Arsenic/FinalAbsPDF/ruppert.pdf.

Sachsenhofer, R.F., Privalov, V.A., Zhykalyak, M.V., Bueker, C., Panova, E., Rainer, T., Shymanovskyy, V.A., Stephenson, R., 2002. The Donets Basin (Ukraine/Russia): coalification and thermal history. Int. J. Coal Geol. 49, 33–55.

Shulga, V.F., 1981. Lower Carboniferous Coal Formations of the Donets Basin (in Russian). Nauka, Moscow. 176 pp.

Stephenson, R.A., Stovba, S.M., Starostenko, V.I., 2001. Pripyat–Dniepr–Donets Basin: implications for dynamics of rifting and the tectonic history of the northern Peri-Tethyan platform. In: Ziegler, P.A., et al. (Eds.), Peri-Tethyan Rift/Wrench Basins and Passive Margins. Peri-Tethys Memoir 6, vol. 186. Mémoires du Muséum National d´Histoire Naturelle, Paris, pp. 369–406.

Sterlin, B.P., Makridin, V.P., Lutsky, P.I., 1963. Stratigraphy of Mesozoic and Cenozoic deposits of the Donets Basin (in Russian). Geology of Coal and Oil Shale Deposits of the USSR 1. Nedra, Moscow, pp. 64–88.

Stovba, S.M., Stephenson, R.A., 1999. The Donbas Foldbelt: its relationships with the uninverted Donets segment of the Dniepr–Donets Basin, Ukraine. Tectonophysics 313, 59–83.

Teichmüller, M., Durand, B., 1983. Fluorescence microscopical rank studies on liptinites and vitrinites in peat and coals, and comparisons with results of the Rock-Eval pyrolysis. Int. J. Coal Geol. 2, 197–230.

Tissot, B.T., Welte, D.H., 1984. Petroleum Formation and Occurrences, 2nd ed. Springer, Berlin. 699 pp.

Triplett, J., Filippov, A., Pisarenko, A., 2001. Coal Mine Methane in Ukraine: opportunities for production and investment in the Donetsk Coal Basin. Report for the U.S. Environmental Protection Agency. http://www.epa.gov/coalbed/pdf/ukraine_handbook.pdf. 127 pp.

Uziyuk, V.I., Ginzburg, A.I., Inosova, K.I., Lapteva, A.M., Fokina, E.I., 1972. Coal petrography method for correlation of sections (in Russian). In: Makedonov, A.V. (Ed.), Correlation of Coalbearing Sediments and Coal Seams in the Donets Basin. Nauka, Leningrad, pp. 24–48.

Van der Zwan, C.J., 1981. Palynology, phytogeography and climate of the lower Carboniferous. Palaeogeogr. Palaeoclimatol. Palaeoecol. 33, 279–310.

Van der Zwan, C.J., Boulter, M.C., Hubbard, R.N.L.B., 1985. Climatic change during the lower Carboniferous in Euramerica, based on multivariate statistical analysis of palynological data. Palaeogeogr. Palaeoclimatol. Palaeoecol. 52, 1–20.

Veld, H., Fermont, W.J.J., Jegers, L.F., 1993. Organic petrological characterization of Westphalian coals from The Netherlands: correlation between *T*max, vitrinite reflectance and hydrogen index. Org. Geochem. 20, 659–675.

Volkman, J.K., Maxwell, J.R., 1986. Acyclic isoprenoids as biological markers. In: Johns, R.B. (Ed.), Biological Markers in the Sedimentary Record. Elsevier, Amsterdam, pp. 1–42.

Volkova, I.B., 1975. The types of coal seams of Carboniferous and their distribution over the territory of the USSR. C. R. 7th Int. Conf. Stratigraphy and Geol. Carboniferous IV, Krefeld, pp. 327–341.

Wüst, R.A.J., Hawke, M.I., Bustin, R.M., 2001. Comparing maceral ratios from tropical peatlands with assumptions from coal studies: do classic coal petrographic interpretation methods have to be discarded? Int. J. Coal Geol. 48, 115–132.

Yablokov, V.S., Bogoljubova, L.I., Kalinenko, V.V., Inosova, K.I., Ishcenko, A.M., 1955. Atlas of Microstructures in Donets Basin Coal (in Russian). Akademia Nauk SSSR, Moscow. 41 pp.

Zaritsky, P.V., 1972. Intracoal kaolinitic layers (tonsteins) (in Russian). In: Makedonov, A.V. (Ed.), Correlation of Coalbearing Sediments and Coal Seams in the Donets Basin. Nauka, Leningrad, pp. 66–71.

Zaritsky, P.V., 1985. Concretions and Values of Their Studying for Solving Questions in Coal Geology and Lithology. Visha Shkola Publ., Kharkov, p. 177. In Russian.

Zhemtchuzhnikov, Yu.A., Yablokov, V.S., Bogolyubova, L.I., Botvinkina, L.N., Feofilova, A.P., Ritenberg, M.I., Timofeev, P.P., Timofeeva, Z.V., 1960. Structure and conditions of formation for main coal-bearing suites and coal seams of the mid-Carboniferous of the Donets Basin. Trans. Geol. Inst. Acad. Sci. U.S.S.R. 15.

Zhykalyak, M.V., Privalov, V.A., 2002. Coal and coal gas resources of the Donets Basin (Ukraine) and their geological characterisation. In: Dusar, M., Devleeschouwer, X. (Eds.), 5th European Coal Conference, Programme and Abstracts, PASS, Mons-Frameries, pp. 156–157.